The quail genome: insights into social behaviour, seasonal biology and infectious disease response

Katrina M. Morris, Matthew M. Hindle, Simon Boitard, David W. Burt, Angela F. Danner, Lel Eory, Heather L. Forrest, David Gourichon, Jerome Gros, Ladeana W. Hillier, et al.

▶ **To cite this version:**

Katrina M. Morris, Matthew M. Hindle, Simon Boitard, David W. Burt, Angela F. Danner, et al.. The quail genome: insights into social behaviour, seasonal biology and infectious disease response. BMC Biology, 2020, 18 (1), Non paginé. 10.1186/s12915-020-0743-4 . hal-02625167

HAL Id: hal-02625167
https://hal.inrae.fr/hal-02625167

Submitted on 26 May 2020

HAL is a multi-disciplinary open access archive for the deposit and dissemination of scientific research documents, whether they are published or not. The documents may come from teaching and research institutions in France or abroad, or from public or private research centers.

L'archive ouverte pluridisciplinaire **HAL**, est destinée au dépôt et à la diffusion de documents scientifiques de niveau recherche, publiés ou non, émanant des établissements d'enseignement et de recherche français ou étrangers, des laboratoires publics ou privés.

Distributed under a Creative Commons Attribution 4.0 International License

Morris et al. BMC Biology (2020) 18:14
https://doi.org/10.1186/s12915-020-0743-4

BMC Biology

RESEARCH ARTICLE Open Access

The quail genome: insights into social behaviour, seasonal biology and infectious disease response

Katrina M. Morris[1*], Matthew M. Hindle[1], Simon Boitard[2], David W. Burt[3], Angela F. Danner[4], Lel Eory[1], Heather L. Forrest[4], David Gourichon[5], Jerome Gros[6,7], LaDeana W. Hillier[8], Thierry Jaffredo[9], Hanane Khoury[9], Rusty Lansford[10], Christine Leterrier[11], Andrew Loudon[12], Andrew S. Mason[1], Simone L. Meddle[1], Francis Minvielle[13], Patrick Minx[8], Frédérique Pitel[2], J. Patrick Seiler[4], Tsuyoshi Shimmura[14], Chad Tomlinson[8], Alain Vignal[2], Robert G. Webster[4], Takashi Yoshimura[15], Wesley C. Warren[16] and Jacqueline Smith[1]

Abstract

Background: The Japanese quail (*Coturnix japonica*) is a popular domestic poultry species and an increasingly significant model species in avian developmental, behavioural and disease research.

Results: We have produced a high-quality quail genome sequence, spanning 0.93 Gb assigned to 33 chromosomes. In terms of contiguity, assembly statistics, gene content and chromosomal organisation, the quail genome shows high similarity to the chicken genome. We demonstrate the utility of this genome through three diverse applications. First, we identify selection signatures and candidate genes associated with social behaviour in the quail genome, an important agricultural and domestication trait. Second, we investigate the effects and interaction of photoperiod and temperature on the transcriptome of the quail medial basal hypothalamus, revealing key mechanisms of photoperiodism. Finally, we investigate the response of quail to H5N1 influenza infection. In quail lung, many critical immune genes and pathways were downregulated after H5N1 infection, and this may be key to the susceptibility of quail to H5N1.

Conclusions: We have produced a high-quality genome of the quail which will facilitate further studies into diverse research questions using the quail as a model avian species.

Keywords: *Coturnix japonica*, Quail, Genome, Influenza, Seasonality, Photoperiod, Bird flu, H5N1

Background

Japanese quail (*Coturnix japonica*) is a migratory bird indigenous to East Asia and is a popular domestic poultry species raised for meat and eggs in Asia and Europe. Quail have been used in genetics research since 1940 [1] and are an increasingly important model in developmental biology, behaviour and biomedical studies [2]. Quail belong to the same family as chickens (Phasianidae) but have several advantages over chickens as a research model. They are small and easy to raise, have a rapid growth rate and a short life cycle, becoming sexually mature only 7 to 8 weeks after hatching [3]. Quail are key for comparative biology research among Galliformes, showing key differences to chickens and other model fowl species, including migratory and seasonal behaviour and immune function [2].

Quail have become a key model in several research fields [4]. The avian embryo has long been a popular model for studying developmental biology due to the accessibility of the embryo, which permits fate mapping studies [5, 6] and dynamic imaging of embryogenesis [7–9]. Several transgenic lines that express fluorescent proteins now exist, which greatly facilitates time-lapse imaging and tissue transplantation [7, 10–13].

* Correspondence: katrina.morris@roslin.ed.ac.uk
[1]The Roslin Institute and R(D)SVS, University of Edinburgh, Easter Bush, Midlothian EH25 9RG, UK
Full list of author information is available at the end of the article

© The Author(s). 2020 **Open Access** This article is distributed under the terms of the Creative Commons Attribution 4.0 International License (http://creativecommons.org/licenses/by/4.0/), which permits unrestricted use, distribution, and reproduction in any medium, provided you give appropriate credit to the original author(s) and the source, provide a link to the Creative Commons license, and indicate if changes were made. The Creative Commons Public Domain Dedication waiver (http://creativecommons.org/publicdomain/zero/1.0/) applies to the data made available in this article, unless otherwise stated.

The quail embryo survives manipulation and culture better than chicken embryos making them ideal for this type of research [3]. Quail have been used as a model for stem cell differentiation, for example a culture system that mimics the development of haematopoietic stem cells has been recently developed, as quail show greater cell multiplication in these cultures than chickens [14].

Quail are also used to study the genetics underlying social behaviours [15], sexual behaviour [16, 17], pre- and post-natal stress programming [18] and emotional reactivity [19–22]. Japanese quail have a fast and reliable reproductive response to increased photoperiod, making them an important model species for investigation into seasonal behaviour and reproduction in birds [23–25]. The molecular mechanisms behind seasonality including metabolism and growth, immunity, reproduction, behaviour and feather moult is poorly understood despite its importance in the management of avian species.

Quail are also important in disease research [26]. Different strains of quail have been developed as models of human disease such as albinism [27] or necrotizing enterocolitis in neonates [28]. Quail lines have also been selected on their immunological response [29]. There are key differences in the immunogenetics of quail and chicken—particularly in the major histocompatibility complex (MHC) [30, 31]. Investigating the immunology of quail is important for understanding infectious disease spread and control in poultry. For example they are an important species for influenza transmission, with previous research showing that quail may play a key role as an intermediate host in evolution of avian influenza [32–34]. Zoonotic H5N1 influenza strains have crossed from quail to human causing mortality in the past [35, 36], making them a potential pandemic source.

We have produced a high-quality annotated genome of the Japanese quail (*Coturnix japonica*) and herein describe the assembly and annotation of the quail genome and demonstrate key uses of the genome in immunogenetics, disease, seasonality and behavioural research demonstrating its utility as an avian model species.

Results

Genome assembly and annotation

Using an Illumina HiSeq 2500 instrument, we sequenced a male *Coturnix japonica* individual from a partially inbred quail line ($F > 0.6$), obtained through four generations of full-sib mating from a partially inbred base population. Total sequence genome input coverage of Illumina reads was ~ 73×, using a genome size estimate of 1.1 Gb. Additionally, 20× coverage of long PacBio reads were sequenced and used to close gaps. The male genome *Coturnix japonica* 2.0 was assembled using ALLPATHS2 software [37] and is made up of a total of 2531 scaffolds (including single contigs with no scaffold association) with an N50 scaffold length of 2.9 Mb (N50 contig length is 511 kb). The assembly sequence size is 0.927 Gb with only 1.7% (16 Mb) not assigned to 33 total chromosomes. *Coturnix japonica* 2.0 assembly metrics were comparable to previous assemblies of Galliformes, and superior to other genomes of other quail species [38, 39] in ungapped (contigs) sequence length metrics (Table 1). Specifically, in comparison to recently published genomic data from the Japanese quail [39], our genome is substantially less fragmented (contig N50 of 0.511 Mb vs 0.027 Mb), has been assigned to more chromosomes and has more complete annotation with ncRNA, mRNA and pseudogenes predicted. Our estimate of total interspersed repetitive elements was 19% genome-wide based on masking with Windowmasker [40]. In the genomes of other quail species, the estimated repeat content was much lower, ~ 10% less in both species [38].

To improve the quantity and quality of data used for the annotation of the genome, we sequenced RNA extracted from seven tissues sampled from the same animal used for the genome assembly. Using the same inbred animal increases the alignment rate and accuracy. The amount of data produced for annotation from the 7 tissues is (in Gb) as follows: 18.9 in brain, 35.6 in heart, 19.3 in intestine, 27.8 in kidney, 39.0 in liver, 18.8 in lung and 34.0 in muscle. High sequencing depth was aimed for in these tissues, to help detect low expression genes including those that are tissue-specific. In total, we predicted 16,057 protein-coding genes and 39,075 transcripts in the

Table 1 Representative assembly metrics for sequenced Galliform genomes

Common name	Assembled version	N50 contig (Mb)	N50 scaffold (Mb)	Total assembly size (Gb)	Assembled chromosomes
Japanese quail	*Coturnix japonica* 2.0	0.511	3.0	0.93	33
Japanese quail	Wu et al. PMID: 29762663	0.027	1.8	0.90	30
Chicken	*Gallus gallus* 5.0	2.895	6.3	1.20	34
Scaled quail	ASM221830v1	0.154	1.0	1.01	NA
Northern bobwhite	ASM59946v2	0.056	2.0	1.13	NA
Turkey	Turkey 5.0	0.036	3.8	1.13	33

All species-specific assembly metrics derived from the NCBI assembly archive

Coturnix japonica genome (Table 2). In comparison to other assembled and annotated Galliformes, transcript and protein alignments of known chicken RefSeq proteins to *Coturnix japonica* suggest the gene representation is sufficient for all analyses described herein (Table 3). However, we find ~ 1000 fewer protein-coding genes in the Japanese quail than the northern bobwhite (*Colinus virginianus*) and scaled quail (*Callipepla squamata*) genomes [38]. We attribute this to the use of different gene prediction algorithms, and the slightly lower assembled size of Japanese quail, 927 Mb compared to 1 Gb in other quail genomes [38] (Table 1).

For further annotation, a set of genes unnamed by the automated pipeline were manually annotated. As part of an ongoing project to investigate hemogenic endothelium commitment and HSC production [14], transcriptomes were produced for two cultured cell fractions. Study of these cells is critical for developmental biology and regenerative medicine, and quail are an excellent model for studying these as they produce much more haematopoietic cells than similar chicken cultures. Approximately 8000 genes were expressed in these cells lines which lacked gene names or annotation from the automated annotation pipeline. Using BLAST [41] searches to identify homology to other genes, 3119 of these were manually annotated (Additional file 1).

Genome completeness was also quantitatively assessed by analysing 4915 single-copy, orthologous genes derived from OrthoDB v7 and v9 [42]. Presence and contiguity of these conserved, avian-specific genes were tested with BUSCO v3.0.2 [43]. A comparison with the chicken assembly [44] (*Gallus gallus* 5.0) indicates that 95% of these genes are present and full length in all three assemblies. The percentage of duplicated, fragmented and missing genes are also very similar between the assemblies (Additional file 2: Figure S1). The quail genome has 10 more missing and 23 more fragmented genes than the *Gallus gallus* 5.0 assembly. However, relative to the total number of genes in the benchmarking set, these increases amount to just 0.2% and 0.5%, respectively. This indicates that the quail genome, like the chicken genome, is highly contiguous and, in terms of its expected gene content, is close to complete.

Galliforme genome synteny

Comparative mapping of the quail and chicken genomes revealed a high conservation of the chromosomal arrangement (Fig. 1; Additional file 3), with no major rearrangements since the divergence of the two species approximately 23 MYA [45]. All identified quail chromosomes showed synteny conservation to their chicken chromosomal counterparts. By comparison, the turkey (*Meleagris gallopavo*) genome is more highly rearranged with two chromosomes having synteny conservation to each of chicken and quail chromosomes 2 and 4 [46]. No large intra-chromosomal translocations were seen between chicken and quail chromosomes, compared to the two seen in the turkey [46, 47]. Inversions and inter-chromosomal translocations were common, with 33 large (> 1 Mb) inversions or translocations occurring between chicken and quail chromosomes (Fig. 1; Additional file 3). The quail chromosomes are more compact than their chicken and turkey counterparts (14% smaller on average). This may be linked to the metabolic cost of migratory flight in quails, as previous studies have demonstrated smaller genomes and higher deletion rates in flying birds compared to flightless birds [48].

Orthologous genes between quail and closely related species were identified through reciprocal BLAST searches. One-to-one orthologs in chicken were identified for 78.2% of all quail genes and 91.8% of protein-coding quail genes (Additional file 4), indicating a high degree of genic conservation in the quail genome. Fewer orthologs were seen between turkey and quail genes (69.3%), although the number of orthologs of protein-coding genes was similar (91.7%), so the discrepancy is likely due to missing non-coding gene predictions in the turkey genome. As expected, conservation of one-to-one orthologs was lower with the mallard duck (*Anas platyrhynchos*), with duck orthologs identified for 64.5% of quail genes (78.9% protein-coding genes).

Endogenous retroviruses (ERVs)

ERVs represent retroviral integrations into the germline over millions of years and are the only long terminal repeat (LTR) retrotransposons which remain in avian genomes [49, 50]. While the majority of ERVs have been degraded or epigenetically silenced, more recent integrations retain the ability to produce retroviral proteins, impacting the host immune response to novel exogenous infections [51, 52]. A total of 19.4 Mb of the *Coturnix japonica* 2.0 assembly was identified as ERV

Table 2 Representative gene annotation measures for assembled Galliform genomes

Common name	Assembled version	Protein-coding genes	Total ncRNA	mRNAs
Japanese quail	*Coturnix japonica* 2.0	16,057	4108	39,075
Japanese quail	Wu et al. PMID: 29762663	16,210	NA	NA
Chicken	*Gallus gallus* 5.0	19,137	6550	46,334
Turkey	Turkey 5.0	18,511	8552	33,308

All species-specific gene annotation metrics derived from the NCBI RefSeq database

Table 3 Estimates of gene and protein representation for sequenced Galliform genomes

		Transcript[1]		Protein[2]	
Common name	Assembled version	Average % identity	Average % coverage	Average % identity	Average % coverage
Japanese quail	*Coturnix japonica* 2.0	93.4	96.2	80.0	85.0
Chicken	*Gallus gallus* 5.0	90.4	84.3	78.0	84.6
Turkey	Turkey 5.0	NA	NA	80.7	80.1

[1]Predicted transcripts per species aligned to Aves known RefSeq transcripts ($n = 8776$)
[2]Predicted proteins per species aligned to Aves known RefSeq ($n = 7733$)

sequence using the LocaTR pipeline [49] (Additional file 5 and Additional file 6). ERVs therefore account for 2.1% of the quail genome sequence, levels similar to those in the chicken and turkey [44] (Additional file 7), and similarly analysed passerine birds [49].

The majority of ERV sequences in all three genomes were short and fragmented, but 393 intact ERVs were identified in the quail, most of which were identified as alpha-, beta- or gamma-retroviral sequences by reverse transcriptase homology. It is possible that the smaller genome size of the quail compared to other birds reflects a more limited expansion of ERVs and other repeats (such as the LINE CR1 element; Additional file 7) within the genome, following the basal avian lineage genome contraction [48, 50]. However, ERV content is highly species-specific [49].

Despite variation in total and intact ERV content, the overall genomic ERV distribution in these three gallinaceous birds was highly similar. ERV sequence density was strongly correlated with chromosome length on the macrochromosomes and Z chromosome ($r > 0.97$; $P < 0.001$), but there was no significant correlation across the other smaller chromosomes. Furthermore, ERV density on each Z chromosome was at least 50% greater than would be expected on an autosome of equal length. These results support the depletion of repetitive elements in gene dense areas of the genome, and the persistence of insertions in poorly recombining regions, as was seen in the chicken [49]. This is further supported by the presence of clusters of intact ERVs (where density was five times the genome-wide level) on the macrochromosomes and sex chromosomes (Additional file 7).

Selection for social motivation

Quail has been used as a model to study the genetic determinism of behaviour traits such as social behaviours and emotional reactivity [21, 22, 53], these being major factors in animal adaptation. Moreover, quail selected with a low social motivation behave in a way that can be related to autistic-like traits, so the genes and causal variants are of wider interest to the biomedical community. Here we use the new quail genome assembly to improve previous results on the detection of selection signatures in lines

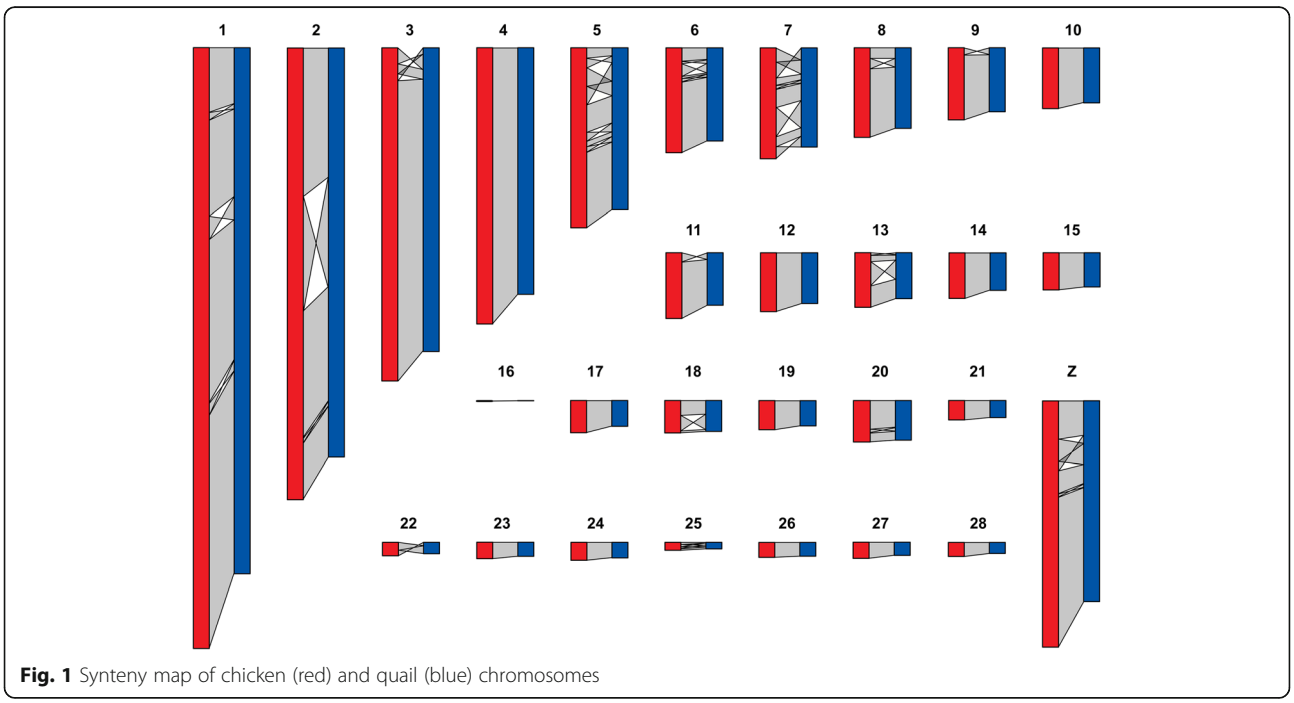

Fig. 1 Synteny map of chicken (red) and quail (blue) chromosomes

selected for sociability. Due to the non-availability of a useable quail reference genome at the start of these studies, genomic sequence data produced from two DNA pools of 10 individuals each from two quail lines diverging for social motivation had been aligned to the chicken reference genome, GallusWU2.58 [54]. As a result, only 55% of the reads had mapped in proper pairs, whereas by using our quail genome as a reference, this number increased to 92%. This corresponds to an improvement of the averaged coverage from 9× to 20× and of the number of analysed SNPs from 12,364,867 to 13,506,139.

The FLK [55] and local [54] score analysis led to the detection of 32 significant selection signature regions ($p < 0.05$) (Additional file 8); Additional file 2: Figure S2 shows an example of such a region on Chr20. This represents a substantial improvement in the number of detected regions, compared with the 10 regions obtained when using the chicken genome as a reference [54]. Of the 32 detected regions, six may be merged in pairs due to their physical proximity, four regions map to new linkage groups absent in the previous analysis, and eight correspond with results obtained in the previous study (Additional file 8). Altogether, 17 new regions were detected. Of these, eight could be seen in the previous analysis, but had not been considered as they did not reach the significance threshold, and nine are solely due to the availability of our quail assembly. Two very short selection signatures previously detected using the chicken assembly as reference are not recovered here and were most probably false positives.

These results confirm the selection signature regions harbouring genes involved in human autistic disorders or being related to social behaviour [54] (*PTPRE*, *ARL13B*, *IMPK*, *CTNNA2*). Among the genes localised in the newly detected genomic regions, several have also been shown to be implicated in autism spectrum disorders or synaptogenic activity (Additional file 8): mutations in the *EEF1A2* gene (eukaryotic elongation factor 1, alpha-2) have been discovered in patients with autistic behaviours [56]; *EHMT1* (Euchromatin Histone Methyltransferase 1) is involved in autistic syndrome and social behaviour disorders in human and mouse [56–59]; *LRRTM4* (Leucine Rich Repeat Transmembrane Neuronal 4) is a synapse organising protein, member of the *LRRTM* family, involved in mechanisms underlying experience-dependent synaptic plasticity [60].

A model for avian seasonal biology

Quail is an important model for studying seasonal biology. Seminal work in quail established that pineal melatonin [61, 62] is regulated by the circadian clock [63]. In mammals, photo-sensing is dependent on a single retinal photoreceptor melanopsin (*OPN4*) that regulates pineal melatonin release. Nocturnal melatonin is critical for mammalian neuroendocrine response to photoperiod and is likely to target melatonin receptors in the *pars tuberalis* [64] (PT). Birds have a distinct non-retinal mechanism for photoreception through deep-brain photoreceptors [65] and melatonin does not appear to be critical for most avian seasonal cycles [66]. The medial basal hypothalamus (MBH) seems to be a critical region for avian perception of photoperiod [67]. There are currently three main candidates for avian deep-brain photoreceptors that communicate the photoperiod signal to seasonal cycles: *OPN4* [68], neuropsin [69] (*OPN5*) and vertebrate ancient [70] (*VA*).

While melatonin may not be a critical component to avian photoperiod signal transduction, it may play a role. Photoperiodic regulation of gonadotropin-inhibitory hormone (GnIH), first identified in quail, has been shown to be regulated by melatonin [71]. Melatonin receptors are also located in the quail PT [72], and like the mammalian PT [73], the expression of core clock genes in the quail PT [74] are phase-shifted with photoperiod. Previously, two studies [67, 75] have examined temperature-dependent effects of photoperiod on core clock genes, *TSHβ* in the PT and *DIO2* and *DIO3* in the MBH. Here, we leverage the new quail genome for genome-wide analysis to determine how photoperiod and temperature interact to determine the MBH transcriptome (Fig. 2a).

We examined the effect of short- (SD) and long-day (LD) photoperiod (SD, 6L18D & LD, 20L4D) and temperature (9 °C and 23 °C) at 12 h after light on (ZT18) (Fig. 2a; Additional file 2: Figure S3) on genome-wide transcription and identified 269 significantly differentially expressed genes (DEGs; FDR < 0.05, log2FC > 1; Additional file 9). A total of 127 DEGs were regulated irrespective of temperature, 60 and 82 DEGs were specific to the contrast with SD 9 °C and 23 °C, respectively. As a single time point was sampled at ZT18, the differential expression reported inevitably captures both circadian effects, such as shifts in phase/period/amplitude, and photoperiod-dependent effects. Resolving photoperiod responses and circadian effects would require a longer time-series with samples across 24 h. Additionally, photoperiod-dependent effects include both acute and expression dependent on the photoperiod history. The ZT18 time point in LD is 12 h after dark and 2 h before dark in SD, so may include acute light-dark photoperception.

We identified 16 temperature-dependent DEGs with a large modulating effect of temperature (log2FC > 1) (Fig. 2e). With the exception of aldehyde dehydrogenase (*ALDH1A1*), the temperature-dependent photoperiod effected DEGs were downregulated in LD. There was an equal division of genes between temperature-dependent amplification and suppression of LD downregulated genes.

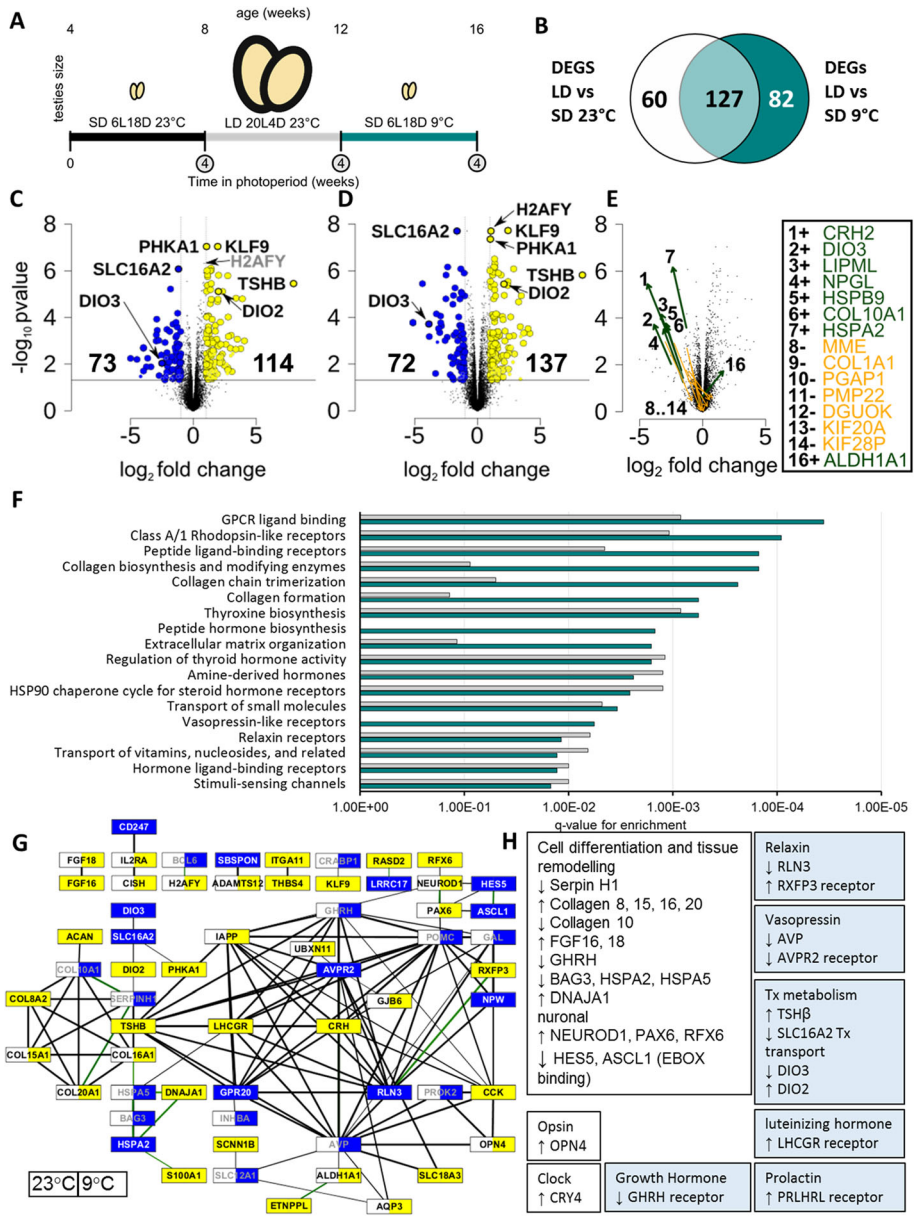

Fig. 2 Genome-wide analysis of temperature-dependent transcriptome responses to photoperiod in quail. Experimental design showing the 3 time-points each sampled after 4 weeks of the target photoperiod (circled) with RNA-Seq at $n = 4$ **a**. Intersection of DEGs between LD 23 °C vs SD 23 °C and LD 23 °C vs SD 9 °C **b**. Volcano plots comparing LD 23 °C vs SD 23 °C showing 71 up (yellow) and 42 down (blue) DEGs **c** and LD 23 °C vs SD 23 °C **d**. Grey labels do not pass fold change threshold at 23 °C. Temperature-dependent effects on fold change in DEGs when comparing SD at 23 °C and SD 9 °C. Arrows point from 23 to 9 °C and indicate a significant amplifying (green) or dampening (orange) effect of 9 °C on photoperiod response **e** significantly enriched pathways in DEG genes at LD vs SD 23 °C (grey) and LD vs SD 9 °C (teal) *q*-value thresholds **f**. Network of up (yellow), down (blue) and no significant change (white) regulated inter-connected genes (LD vs SD) using the String database. The left side of a node indicates the expression change at 23 °C and right at 9 °C. Edges are weighted by the combined score, and green edges represent experimental support **g**. Summary of upregulated and downregulated pathways **h**

The MBH shows strong TSHβ induction in LD (Fig. 2c, d, log2FC = 7.96 at 9 °C, 8.36 at 23 °C), indicating the stamp contains the adjacent PT as well as the MBH. Previous in situ data [75] support the localisation of TSHβ in the quail PT. Consistent with previous MBH findings [75], we observed significant upregulation of *DIO2* and downregulation of *DIO3*, in LD. We also observed a significant effect of cold (9 °C) in short days as an amplifier of *DIO3* LP downregulation (Fig. 2e, log2FC = − 3.86 at 9 °C, − 2.51 at 23 °C). We were unable to confirm any significant effect of cold on *DIO2*. We note significant photoperiod-dependent downregulation of the thyroid

hormone-specific transporter *SLC16A2* in LP that was amplified at 9 °C (log2FC = − 1.19 at 9 °C, − 1.63 at 23 °C).

Differential regulation of G-protein coupled receptor (GPCR) signalling was the most enriched pathway regulated by photoperiod (Fig. 2f; Additional file 10). It also emerged as the largest connecting component within the String interaction network of DEG genes (Fig. 2g). TSHβ itself binds to the GPCR THR [76]. G-protein signalling is also critical for opsin signalling [77]. We also observed transcriptional regulation in other GPCR hormone receptors, including Relaxin, Vasopressin, LH, Prolactin and GH. GnRH is associated with VA opsins in AVT neurones and has been suggested as a photoperiod sensor [70]. We also noted downregulation of the neuronally important GPCR GPR20 (Fig. 2g). In mice, deficiency of GPR20 is associated with hyperactivity and may play a role in cAMP-dependent mitogenesis [78]. There was a strong enrichment of collagen biosynthetic processes and extracellular matrix organisation processes (Fig. 2f) and a large body of genes associated with cell differentiation and development (Fig. 2h).

We observed photoperiod-dependent regulation of a single clock gene, *CRY4*. *CRY4* is upregulated in LP (log2FC = 0.85 at 23 °C, 1.37 at 9 °C). This is consistent with the finding of Yasuo et al. [67] that the expression of *PER2-3*, *CLOCK*, *BMAL1*, *CRY1-2* and *E4BP4* remain stable across photoperiods. CRY4 has recently been the subject of considerable research in migratory birds [79, 80] and the observed variation across photoperiods in a non-migratory Galliform suggest quail could be an interesting model to further investigate SP-dependent non-migratory CRY4 function in the MBH.

We detected photoperiod effects on *OPN4* transcripts, which were upregulated in LD. Photoperiod-dependent expression in *OPN4* may well play a role in the photoperiod-refractory response. Encephalopsin (*OPN3*) was found to be highly expressed in the MBH (2.31 to 2.42 log2CPM) but without significant changes in expression. OPN3 has recently been identified in the hypothalamus of chick hatchlings [81] but not as yet to the MBH of adult birds. *OPN5* (− 0.46 to 0.89 log2CPM) and *VA* (− 0.11 to 0.31 log2CPM) were also unchanging and expressed at a low level in the MBH sample. These findings confirm the importance of temperature and photoperiod-dependent regulation of thyroid hormone metabolism in the avian MBH (Fig. 3).

Quail immune gene repertoire

We investigated the immune genes in the quail genome in detail due to the importance of quail as a model in disease research. The MHC-B complex of the quail has been previously sequenced and found to be generally conserved compared to chicken in terms of gene content and order [30, 31]. However, the quail MHC contains a higher copy number of several gene families within the MHC-B [30] and shows increased structural flexibility [31], as well as an inversion in the *TAP* region [30]. The MHC-B sequence in the quail genome extends from the previously sequenced scaffold, and this additional region also contains similar gene content and order to chicken, but with gene copy number variations. As in the chicken, the *CD1A* and *B* genes are found downstream of the MHC I region, while many *TRIM* family genes and *IL4I1* are encoded upstream. The BG region, which encodes a family of butrophylin genes known as *BG* genes in the chicken, was also present in the quail. Within this region, six *BG* genes were identified in the quail, compared to 13 in the chicken [82]. At least five of these *BG* genes are transcribed in the quail lung and ileum. The chicken and turkey have an additional MHC locus known as the Rfp-Y or MHC-Y locus, which contains several copies of non-classical MHCI-Y and MHCIIB-Y genes. However, no MHC-Y genes have been previously identified in quail. BLAST searches of both the quail genome and quail transcriptomes, as well as the bobwhite and scaled quail genomes, failed to identify any MHC-Y genes, indicating this locus probably does not exist in the quail.

Cathelicidins and defensins are two families of antimicrobial peptides that have activities against a broad range of pathogens and exhibit immune-modulatory effects. Orthologs of all four chicken cathelicidins and of 13 chicken defensins [83] were identified in the quail genome (Additional file 11). Due to their high divergence, of the 13 defensins, only four were annotated through the annotation pipeline, with the remainder identified through BLAST and HMMer searches with chicken defensins. The only poultry defensin missing from the quail genome is *AvBD7*. The defensins are encoded in a 42 kb cluster on quail chromosome 3, as in chickens. A 4 kb gap in the scaffold in this region may explain the missing *AvBD7* sequence.

Several genes are thought to be crucial for influenza resistance in both humans and birds, including *RIG-I*, *TLR* and *IFITM* genes. *RIG-I* has not previously been identified in chicken, despite being present in ducks and many other bird orders, and is considered highly likely to be deleted from the chicken genome [84]. In addition, an important RIG-I binding protein RNF135 has also not been identified in chicken [85]. Likewise, an ortholog of *RIG-I* or *RNF135* could not be identified in the quail genome or transcriptomes through BLAST and HMMer searches and therefore is likely missing in the quail also. Orthologs of all five chicken *IFITM* genes (*IFITM1, 2, 3, 5* and *10*) were identified in the quail genome and transcriptomes. In addition, orthologs of each chicken toll-like receptors (TLRs), including key TLRs for viral recognition, *TLR4*

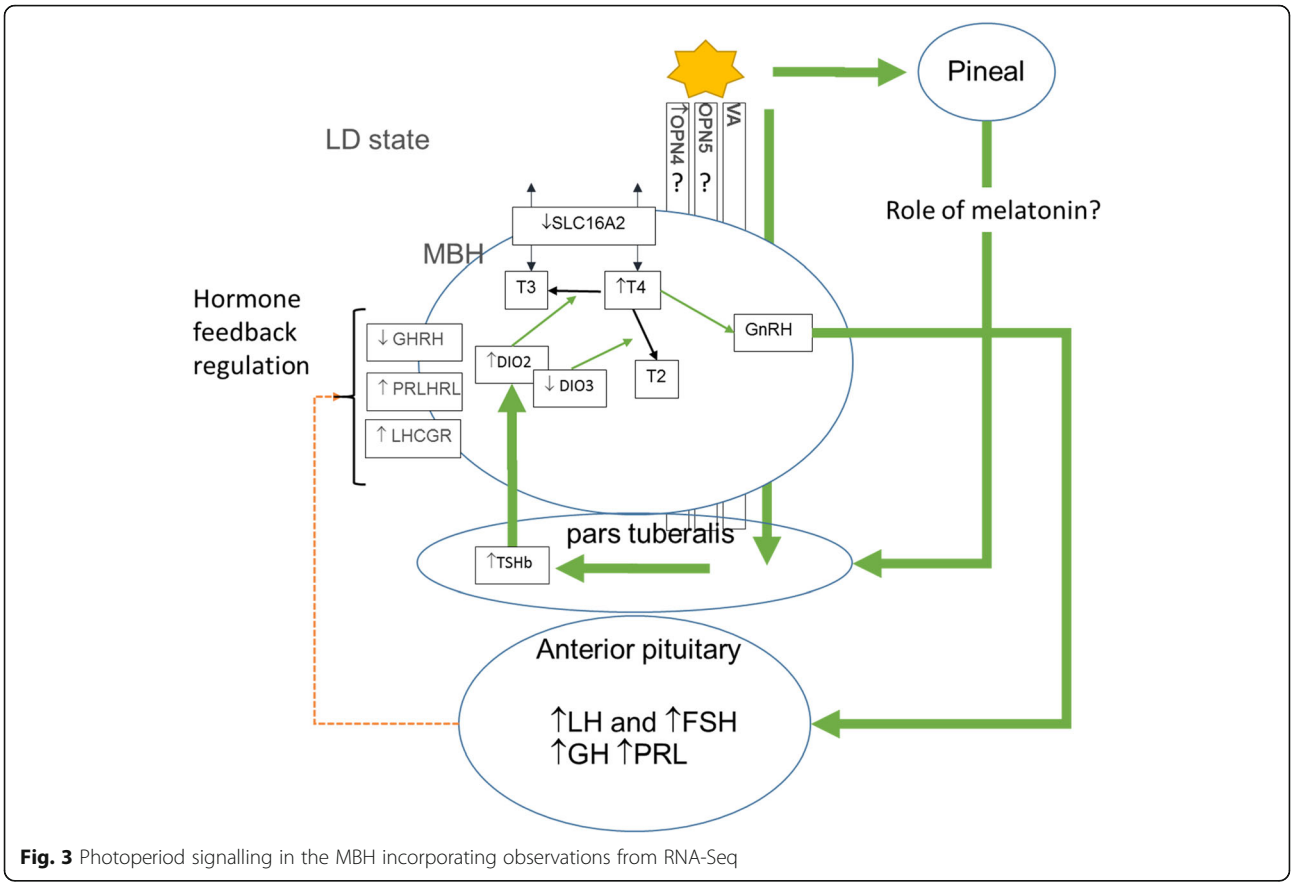

Fig. 3 Photoperiod signalling in the MBH incorporating observations from RNA-Seq

and *TLR7*, were identified in the quail genome, except that of *TLR1A*. *TLR1A* was not identified through BLAST and HMMer searches of the quail genome. In chicken, *TLR1A* and *TLR1B* are located between the genes *KLF3* and *FAM11A1*. However, in the quail genome, there is only one gene at this location. We extracted TLR1-like sequences from other Galliform genomes and Zebrafinch and created a phylogeny with TLR2 and 4 as outgroups (Additional file 2: Figure S4). This phylogeny indicates single highly supported clades of TLR1A and B, indicating that the duplication occurred in an ancestor of Neognathae avians. TLR1A was identified in the other two quail species' genomes. The absence of TLR1A from the quail genome assembly suggests it has been lost from the quail genome, although an assembly error cannot be ruled out.

Quail response to H5N1 influenza

Highly pathogenic influenza A viruses (HPAI), such as strains of H5N1, are responsible for enormous economic losses in the poultry industry and pose a serious threat to public health. While quail can survive infection with low pathogenic influenza viruses (LPAI), they experience high mortality when infected with strains of HPAI [86]. Quail are more susceptible than chickens to infection by some strains of H5N1 including one that caused human mortality (A/Hong Kong/156/97) [36]. Previous research has shown that quail may play a key role as an intermediate host in the evolution of avian influenza, allowing viral strains to spread from wild birds to chickens and mammals [32, 33, 36, 87]. Unlike quail and chicken, aquatic reservoir species such as duck are tolerant of most HPAI strains [88]. The generation of a high-quality quail genome has enabled us to perform a differential transcriptomic analysis of gene expression in quail infected with LPAI and HPAI, to better understand the response of quail to influenza infection. Lung and ileum samples were collected at 1 day post infection (1dpi) and 3 days post infection (3dpi). We also reanalysed previous data collected from duck and chickens [89] and compare this to the quail response.

To provide an overview of the response to LPAI and HPAI in quail, we examined pathway and GO term enrichment of DEGs (see Additional file 12, Additional file 13 and Additional file 2; Figures S5-S8). In response to LPAI infection, pathways enriched in the ileum included metabolism, JAK/STAT signalling, IL6 signalling and regulation of T cells (Additional file 2: Figure S5). In the lung, pathways upregulated included complement, IL8 signalling and leukocyte activation (Additional file 2: Figure S6). In the

lung at 3dpi, highly enriched GO terms included "response to interferon-gamma", "regulation of NF-kappaB", "granulocyte chemotaxis" and "response to virus" (Additional file 2: Figure S7), which are key influenza responses. This indicates an active immune response occurs to LPAI infection in quail, involving both ileum and lung, but with the strongest immune response occurring in the lung.

Genes upregulated in response to HPAI in the ileum were related to metabolism and transport, while inflammatory response was downregulated at 1dpi (Additional file 2: Figure S7). Downregulated pathways at 1dpi included IL-6, IL-9 and neuro-inflammation signalling pathways (Additional file 2: Figure S7). In the quail lung, many genes were downregulated after HPAI infection (Additional file 12). At 3dpi, most downregulated pathways and terms were linked to immune system processes. GO terms with the highest fold enrichment in downregulated genes at this time included T and B cell proliferation, TNF signalling pathway, TLR pathway and IFN-G production (Additional file 13). Pathways downregulated included both Th1 and Th2 pathways, T cell, B cell and macrophage signalling pathways (Additional file 2: Figure S8). This indicates that crucial immune responses in quail are downregulated in ileum, and particularly in the lung at day 3, following HPAI infection.

To compare the response of quail, duck and chicken, clustering of gene counts was examined using BioLayout 3D [90]. This revealed a cluster of 189 genes that were strongly upregulated at 1dpi in the duck following HPAI infection, which showed no or very low response in chicken and quail (Additional file 14). This cluster was dominated by RIG-I pathway and IFN response genes including *IFNG*, *DDX60*, *DHX58*, *IRF1*, *IRF2* and *MX1*. Pathways associated with this cluster include MHCI processing and death receptor signalling (Additional file 2: Figure S9). Thus, the lack of this early anti-viral response may be key to the susceptibility of Galliformes to HPAI.

To further compare the responses between the three species, enrichment of pathways in each species was examined (Fig. 4; Additional file 2: Figure S10). In LPAI infection, comparison between ileum samples was limited due to low number of DEGs, but in lung, many pathways were shared between the species, primarily immune pathways. In HPAI, pathway analysis revealed very few commonly regulated pathways between the three species. However, at 1dpi in the ileum and 3dpi in the lung, there were many pathways that were downregulated in the quail, not altered in chicken and upregulated in the duck. In the ileum at 1dpi, this included pattern recognition and death receptor signalling. In the lung at 3dpi, this involved host of immune-related pathways including production of NOS by macrophages, pattern recognition, B and T cell signalling and NK-KB, IL8 and IL2 signalling.

The proportion of genes commonly regulated between quail, chicken and duck to LPAI and HPAI infection was also examined (Fig. 5; Additional file 2: Figure S11). The responses to LPAI showed a high level of commonly regulated genes between the three species; for example, 50.5% of chicken DEGs and 42.5% of duck DEGs in lung at day 1 were also differentially expressed in quail. In HPAI, consistent with the heatmap comparison (Fig. 4), the responses of chicken, quail and duck were largely unique, with few genes commonly differentially expressed. There was a large set of genes that were upregulated in duck, while being downregulated in quail at 3dpi, in both ileum and lung. In lung, these genes were related primarily to innate immune system pathways, including pattern recognition pathways, cytokine production, leukocyte adhesion, TNF production, interferon production, B cell signalling and response to virus (Additional file 13). Genes with the greatest differential expression included *RSAD2* which inhibits viruses including influenza, *IFIT5* which senses viral RNA and *OASL* which has anti-viral activity. These differences further highlight that the anti-viral immune response is dysregulated in quail. Additionally in both ileum and lung, the apoptosis pathway was enriched in duck, but not in quail (Additional file 13). Apoptosis is known to be a critical difference in the response of chickens and ducks to HPAI infection [91].

Lastly, we examined the response of key families involved in influenza and immune response, focussing on the lung (Additional file 15). *IFITM* genes have previously been found to have a crucial role in HPAI resistance [89] and may block AIV from entering cells [92]. Consistent with previous findings in the chicken [89], quail showed no significant upregulation of *IFITM* genes, while these genes in duck were strongly upregulated (Additional file 15), TLRs and MHC receptors are involved in recognition of foreign molecules and triggering either an innate (TLR) or adaptive (MHC) immune response. TLR3, 4 and 7, which bind viral RNAs, were upregulated in response to LPAI in quail. A reversal was seen in response to HPAI, with *TLR4* and *7* substantially downregulated. Likewise, genes of both MHC class I and II were upregulated in response to LPAI and downregulated in response to HPAI. By comparison there was no perturbation of TLR and MHC genes in chicken and upregulation of class I genes in duck. The quail seems to have a highly dysfunctional response to HPAI infection with key innate and adaptive immune markers downregulated at 3dpi, which contrasts with the strong immune response mounted by the duck and minimal immune response in the chicken.

Discussion

We have assembled, annotated and analysed a high-quality quail genome. Quails are a crucial model in developmental biology, behaviour and photoperiod research and also

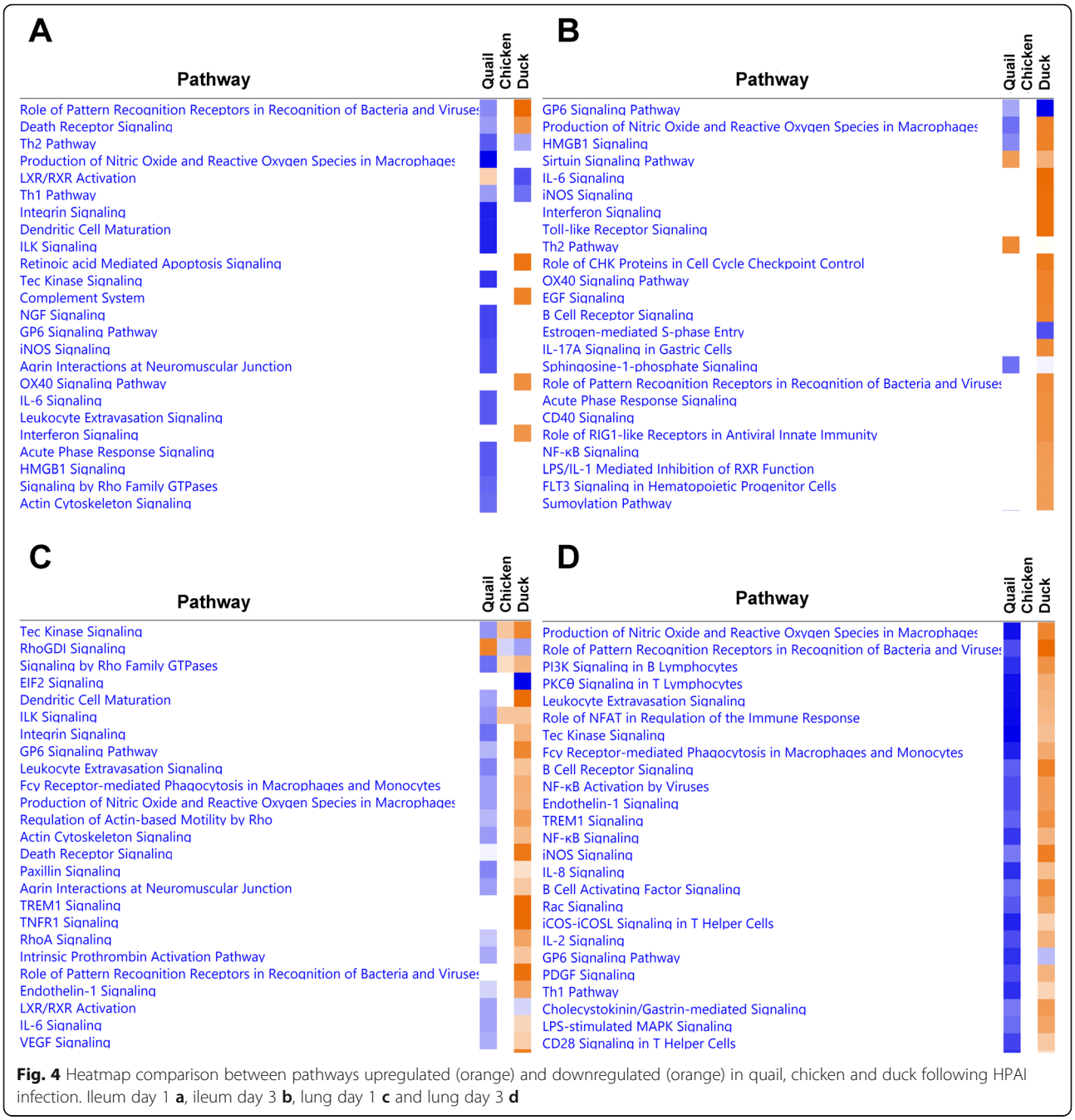

Fig. 4 Heatmap comparison between pathways upregulated (orange) and downregulated (orange) in quail, chicken and duck following HPAI infection. Ileum day 1 **a**, ileum day 3 **b**, lung day 1 **c** and lung day 3 **d**

disease studies. Using this genome, we have made important discoveries in these fields of research.

The quail genome assembly is highly comparable to the chicken genome assembly (*Gallus gallus* 5.0) in terms of contiguity, assembly statistics, annotation, gene content and chromosomal organisation. It is also a superior assembly to other quail family and Galliform genome assemblies. The quail genome shows high conservation to the chicken both in chromosomal synteny, in gene orthology and in ERV genomic density. The immune gene complement in the quail genome is similar to that of chicken but with some important differences, including changes to the MHC including a likely lack of the MHC-Y locus and of the avian *TLR1A* gene.

Quail are used as a model to study the genetics of behaviour, and leveraging the quail genome we examined selection signatures in lines selected for sociability. This confirmed selection on regions harbouring genes known to be involved in human autistic disorders or related to social behaviour. Autistic spectrum disorders are observed in several disorders that have very different aetiology, including fragile X Syndrome, Rett Syndrome or Foetal

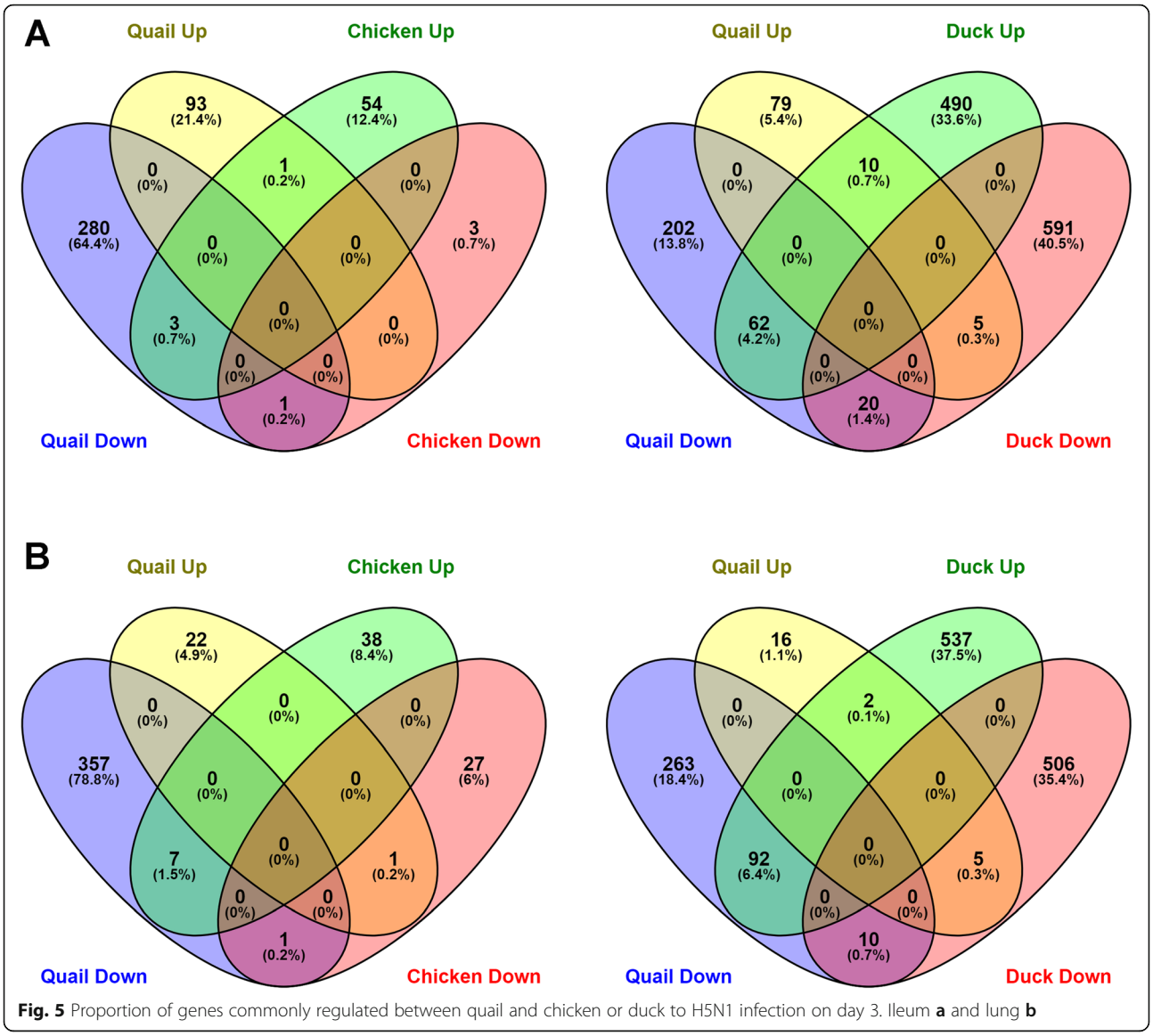

Fig. 5 Proportion of genes commonly regulated between quail and chicken or duck to H5N1 infection on day 3. Ileum **a** and lung **b**

Anticonvulsant Syndrome. While these disorders have very different underlying etiologies, they share common qualitative behavioural abnormalities in domains particularly relevant for social behaviours such as language, communication and social interaction [93, 94]. In line with this, several experiments conducted on high social (HSR) and low social (LSR) reinstatement behaviour quail indicate that the selection program carried out with these lines is not limited to selection on a single response, social reinstatement, but affect more generally the ability of the quail to process social information [18]. Differences in social motivation, but also individual recognition have been described between LSR and HSR quail [95, 96]. Inter-individual distances are longer in LSR quail [95] and LSR young quail have decreased interest in unfamiliar birds [97] and lower isolation distress than HSR ones [20]. Further experiments will be required to examine the possible functional link between the selected genes and the divergent phenotype observed in these lines. Also, by analyses of genes known to be differentially expressed in the zebra finch during song learning, we hope to comparatively understand molecular systems linked to behaviour in the avian brain.

Quail is a key model species for studying seasonal biology. We have added to this body of work by using the quail genome for genome-wide analysis to determine how photoperiod and temperature interact to determine the medial basal hypothalamus transcriptome. We confirm the importance of temperature and photoperiod-dependent regulation of thyroid hormone metabolism in the avian MBH. Temperature-dependent amplification and suppression of the photoperiod response may indicate qualitative differences

in the MBH pathways or simply reflect different stages of progression through seasonally phased processes. This could be further investigated by contrasting across time-series at different temperatures. We also observed concurrent regulation of multiple hormonal signalling pathways, this may reflect a diversity of pathways and cell types in the MBH or reflect a corrective mechanism to account for cross-talk with other GPCR pathways. We observed LH, PRL, and GH receptor transcript changes which may indicate modulation of a GnRH-anterior pituitary feedback mechanism. In addition to observing high *OPN3* expression in the MBH, we also noted LD overexpression of *OPN4*, which could provide a potential component for an avian photoperiod-refractory mechanism. This study demonstrated the utility of genome-wide transcriptome analysis in quail to provide valuable insights and novel hypotheses for avian seasonal biology.

Quails are important for disease research, particularly in influenza where they act as a key intermediate host in the evolution of avian influenza [32–34], allowing viral strains to spread from wild birds to mammals and domesticated chickens. We found that quail have a robust immune response to infection with LPAI, allowing them to survive the infection. However, they show dysregulation of the immune response after infection with HPAI, and this may explain their susceptibility to HPAI strains. Quail, chicken and duck showed similar responses to LPAI. After HPAI infection, while ducks showed a robust immune response, quails did not. This difference may be a result of the higher viral dose the ducks were infected with; however, the lower dose given in chickens and quail still resulted in replicative virus and mortality of all chickens and quails by 5dpi, and therefore should have induced an anti-viral immune response. A more substantial immune response may have developed in the short period between 3dpi and time of death of the quails (between 3 and 4dpi); however, this was too late to prevent mortality. An IFITM response was not seen against HPAI while genes associated with apoptosis were downregulated, mechanisms previously found to be important in resistance to HPAI [89, 91], which potentially allows the virus to easily enter cells and spread early in infection. Anti-viral and innate immune genes, including those involved in antigen recognition, immune system activation and anti-viral responses were downregulated at 3dpi, which would prevent an effective immune response and viral clearance once infection is established. This study provides crucial data that can be used to understand the differing response of bird species to AIV, which will be critical for managing and mitigating these diseases in the future.

Conclusions

Here we describe the assembly, annotation and use of a high-quality quail genome, an important avian model in biological and biomedical research. This genome will be crucial for future comparative avian genomic and evolutionary studies. It provides essential genetic and genomic reference information for making precise primers and nucleic acid probes, and accurate perturbation reagents including morpholinos, RNA inactivation tools, and CRISPR-Cas9 constructs. We have demonstrated the utility of this genome in both infectious disease and behavioural research providing further confirmation of the importance of quail as a research model, and for its role in agricultural and animal health studies. Specifically, the availability of this genome has allowed us to make significant discoveries in the unique response of quail to highly pathogenic avian influenza infection, helping elucidate the basis for extreme susceptibility seen in this species. It has also allowed us to identify and confirm genes and genomic regions associated with social behaviours. Furthermore, we have shown that genome-wide transcriptomics using this genome facilitated further insights and hypothesis into the mechanism of photoperiodism in avian seasonal biology. Moving forward, the availability of a high-quality quail genome will facilitate the study of diverse topics in both avian and human biology including disease, behaviour, comparative genomics, seasonality and developmental biology.

Methods

Whole genome sequencing and assembly

To facilitate genome assembly by avoiding polymorphism, we produced an individual as inbred as possible. We started with a quail line previously selected for early egg production and having a high inbreeding coefficient [98] and four generations of brother-sister matings produced a dedicated line "ConsDD" ($F > 0.6$) (PEAT, INRAE Tours, France). A 15-week-old male *Coturnix japonica* (id. 7356) was then selected from this line for the sequencing project. Genomic DNA was extracted from a blood sample using a high-salt extraction method [99]. Our sequencing plan followed the recommendations provided in the ALLPATHS2 assembler [37]. This model requires 45× sequence coverage of each fragment (overlapping paired reads ~ 180 bp length) from 3 kb paired-end (PE) reads as well as 5× coverage of 8 kb PE reads. These sequences were generated on the HiSeq2500 Illumina instrument. Long reads used for gap filling were generated at 20× coverage on the same DNA source using a RSII instrument (Pacific Biosciences). The Illumina sequence reads were assembled using ALLPATHS2 software [37] using default parameter settings and where possible, and scaffold gaps were closed by mapping and local assembly of long reads using PBJelly [100]. As most scaffold gaps were small, long-read data was only needed to correct around 1 Mb of the assembly. The Illumina long insert paired-end reads (3 kb and 8 kb PE) were

used to further extend assembled scaffolds using SSPACE [101]. The draft assembly scaffolds were then aligned to the genetic linkage map [53] and the Galgal4.0 chicken reference (GenBank accession: GCA_000002315.2) to construct chromosome files following previously established methods [44]. Finally, all contaminating contigs identified by NCBI filters (alignments to non-avian species at the highest BLAST score obtained) and all contigs < 200 bp were removed prior to final assembly submission.

Gene annotation

Specific RNA-Seq data for the genome annotation was produced from the same animal used for the genome assembly. RNA was extracted from heart, kidney, lung, brain, liver, intestine and muscle using Trizol and the Nucleospin® RNA II kit (MACHEREY-NAGEL), following the manufacturer's protocol.

The *Coturnix japonica* assembly was annotated using the NCBI pipeline, including masking of repeats prior to ab initio gene predictions, for evidence-supported gene model building. We utilised an extensive variety of RNA-Seq data to further improve gene model accuracy by alignment to nascent gene models that are necessary to delineate boundaries of untranslated regions as well as to identify genes not found through interspecific similarity evidence from other species. A full description of the NCBI gene annotation pipeline was previously described [102]. Around 8000 lacked gene symbols from this pipeline, and these were further annotated manually by using BLAST searches using the corresponding sequences and extracting protein names from Uniprot.

Comparative analyses

A set of single copy, orthologous, avian-specific genes were selected from OrthoDB v. 9 [42] and their status (present, duplicated, fragment or missing) were tested with BUSCO v.3.0.2 [43] in the *Gallus gallus* 5.0 and *Coturnix japonica* 2.0 genomes. Ab initio gene predictions were done within the BUSCO framework using tBLASTn matches followed by avian-specific gene predictions with Augustus v. 3.3 [103]. Gene status was assessed by running HMMER [104] with the BUSCO HMM profiles of the orthologous sequences. Comparative maps and breakpoint data were generated using AutoGRAPH [105] using chicken and quail gff annotation files, using default settings. The TLR1A phylogeny was constructed in MEGA7 [106] using the Neighbour-Joining method [107].

Endogenous retrovirus identification

Endogenous retroviruses (ERVs) were identified in the *Coturnix japonica* 2.0 and Turkey 5.0 genome assemblies using the LocaTR identification pipeline [49] and compared to a previous analysis of ERVs in the *Gallus gallus* 5.0 genome assembly [44]. LocaTR is an iterative pipeline which incorporates LTR_STRUC [108], LTRharvest [109], MGEScan_LTR [110] and RepeatMasker [111] (http://repeatmasker.org) search algorithms.

Sociability selection study

The data and methods used have been described previously [54]. Briefly, two quail lines were used, divergently selected on their sociability [19]: high social (HSR) and low social (LSR) reinstatement behaviour. A total of 10 individuals from generation 50 of each quail line were sequenced after equimolar DNA pooling. Sequencing was performed (paired-ends, 100 bp) on a HiSeq 2000 sequencer (Illumina), using one lane per line (TruSeq sbs kit version 3). The reads (190,159,084 and 230,805,732 reads, respectively, for the HSR and LSR lines) were mapped to the CoJa2.2 genome assembly using BWA [112], with the mem algorithm. Data are publicly available under SRA accession number SRP047364. Within each line, the frequency of the reference allele was estimated for all SNPs covered by at least 5 reads, using Pool-HMM [113]. This analysis provided 13,506,139 SNPs with allele frequency estimates in the two lines. FLK values [55] were computed for all these SNPs, and the local score method [54] was applied to the p value on single-marker tests.

Photoperiod study

MBH tissue was collected as previously [75]. Male 4-week-old quail were obtained from a local dealer in Japan and kept under SD conditions (6L18D) for 4 weeks. At 8 weeks of age, quail were transferred to LD conditions (20L4D) and kept under LD conditions for 4 weeks to develop their testes. And then, 12-week-old LD quail were transferred to short-day and low-temperature (SL: 6L18D 9C) conditions for another 4 weeks to fully regress their testes. All samples were collected at 18 h after light on (ZT18), which for SD birds is 12 h after dark onset, and for LD birds 2 h before dark onset. (Lights on is same for LD and SD and lights off was extended in LD group). RNA-Seq was performed using a TruSeq stranded mRNA prep (Revision E 15031047) with 125 bp paired-end reads on a HiSeq Illumina 2500 with four replicates in each of the three conditions.

Reads were quality (Phred>25) and adapter trimmed with Trim Galore (version 0.4.5). Tophat (version 2.1.0) [114] with bowtie2 (version 2.2.6) was used to map reads to the quail genome (GCA_001577835.1 *Coturnix japonica* 2.0), using the NCBI annotation. We determined feature counts for gene loci using the featureCounts program [115] in the subread (version 1.5.0) package [116]. Statistical analysis was performed using the limma package [117] (version 3.36.1) in the R programming environment

(version 3.5.0). The trimmed mean of M-values normalisation method (TMM) was used for normalisation with Voom for error estimation (Additional file 2: Figure S3). We retained gene loci with more than 10× coverage in three replicates in at least two conditions. A categorical least squared regression model was fitted using LD 23 °C, SD 23 °C and SD 9 °C conditions. Statistics for pairwise comparisons were then recalculated by refitting contrasts to the model for LD 23 °C vs SD 23 °C, LD 23 °C vs SD 9 °C and SD 23 °C vs SD. The Benjamini-Hochberg approach [118] was used to estimate the false discovery rate. For reporting numbers of photoperiod significant genes, we applied thresholds of FDR < 0.05, log2 CPM > 0 and absolute log2 fold change > 1. Temperature-dependent genes are reported as those with a photoperiod significant effect at either 23 °C or 9 °C and a significant effect when contrasting SD 9 °C and SD 23 °C at the same thresholds defined across photoperiods.

Influenza response study

All experiments involving animals were approved by the Animal Care and Use Committee of St. Jude Children's Research Hospital and performed in compliance with relevant policies of the National Institutes of Health and the Animal Welfare Act. All animal challenge experiments were performed in animal biosafety level 2 containment facilities for the LPAI challenges and in biosafety level 3 enhanced containment laboratories for the HPAI challenges. Viral challenges of quail, tissue collection, RNA extractions and sequencing were carried out as previously described for chicken [89]. Fifteen quail, 15 chickens and 15 ducks were challenged with 10^6 EID_{50} intranasally, intratracheally and intraocularly of LPAI A/Mallard/British Columbia/500/2005 (H5N2) in phosphate buffered saline (PBS). Fifteen quail and 15 chickens were challenged with $10^{1.5}$ EID_{50} intranasally, intratracheally and intraocularly of HPAI A/Vietnam/1203/2004 (H5N1) in PBS. Twelve ducks were challenged with 10^6 EID_{50} intranasally, intratracheally and intraocularly of HPAI A/Vietnam/1203/2004 (H5N1) in PBS. Mock infection control groups for quails ($n = 12$), chickens ($n = 10$) and ducks ($n = 15$) were also inoculated, receiving an equivalent volume of PBS via the same route of administration. Birds were randomly allocated to experimental groups. Oropharyngeal and cloacal swabs were taken from all birds and virus titres are shown in (Additional file 2: Tables S1–3). Animals were monitored daily for clinical signs. Lung and ileum samples were collected from all birds on 1dpi and 3 dpi. RNA extractions were performed using Trizol and QIAGEN's RNeasy kit. For sequencing, 36-cycle single-ended sequencing was carried out on the Genome Analyser IIx using Illumina v3 Sequencing by Synthesis kits.

All quail, as well as duck and chicken RNA-Seq reads from the previous study [89], were analysed as follows: Ileum and lung RNAs were analysed from PBS infected control (3 samples from each of 1dpi and 3dpi), H5N1-infected (3 samples from each of 1dpi and 3dpi, except quail ileum 1dpi which had 2 samples) and H5N2-infected (3 samples from each of 1dpi and 3dpi). A total of 251 million reads of 36 nucleotides in length were generated for quail. Reads were quality checked using FastQC (version 0.11.2) and trimmed for quality using Trim Galore (version 0.4.0). Mapping was performed to the quail genome (GCA_001577835.1 Coturnix_japonica_2.0), chicken genome (GCA_000002315.3 Gallus_gallus-5.0) and duck (GCA_000355885.1 BGI_duck_1.0) using Tophat2 [114] (version 2.1.0) using default options including the default multi-mapping cutoff of 20 locations. Mapping of reads was also performed to H5N1 and H5N2 genomes using Kallisto [119] (version 0.42.4; Additional file 16). For quantification and differential analysis, the following pipeline was used. First, transcripts were assembled and quantified using cufflinks [120], guided with the NCBI annotation for the relevant genome, and the multi-read correct option was used to more accurately estimate abundances of multi-mapped reads. The transcriptomes were merged using stringtie merge [121], and cuffdiff [115] was used for differential analysis using default settings. To determine orthology between quail, duck and chicken genes, reciprocal BLAST searches were performed. For analysis of GO term enrichment, the PANTHER overrepresentation test [122] was used, and for pathway analysis, Ingenuity Pathway Analysis software (QIAGEN) was used. For clustering analysis, BioLayout 3D [90] was used using default settings except 1.4 inflation for Markov clustering.

Supplementary information

The online version of this article (https://doi.org/10.1186/s12915-020-0743-4) contains supplementary material, which is available to authorized users.

Additional file 1. List of unannotated quail genes and their manual annotation

Additional file 2. Supplementary Figures. S1-S11 and Tables S1–3

Additional file 3. Location of breakpoints between chicken and quail chromosomes

Additional file 4. Percent of quail genes with orthologs identified in related bird genomes

Additional file 5. BED file containing location of ERVs in quail genome

Additional file 6. BED file containing location of ERVs in turkey genome

Additional file 7. A comparative summary of assembled ERVs in quail, chicken and turkey

Additional file 8. List of selection signatures detected from the HSR / LSR lines

Additional file 9. Statistics from photoperiod differential expression study

Additional file 10. Pathway analysis from photoperiod study

Additional file 11. Sequences of cathelicidins and defensin genes identified in quail genome

Additional file 12. List of differentially expressed genes, FDR < 0.05 and fold change > 1.6 in infection study

Additional file 13. Overrepresented GO terms in differentially expressed genes in infection study

Additional file 14. List of the cluster of genes upregulated in duck at day 1 during HPAI infection, with the corresponding fold changes in each species. NS = Not significantly differentially regulated

Additional file 15. Regulation of IFITM, MHC and TLR family genes in quail, chicken and duck following HPAI and LPAI infection

Additional file 16. Viral read presence in quail samples

Acknowledgements

The authors would like to thank the Edinburgh Genomics sequencing facility (Edinburgh, UK) and the GeT-Plage platform (http://get.genotoul.fr/en/) for carrying out the transcriptomic sequencing. We thank the McDonnell Genome Institute sequencing production group for all sequencing support to produce the reference genome. We are grateful to the genotoul bioinformatics platform Toulouse Midi-Pyrenees (Bioinfo Genotoul) for providing help, computing and storage for these resources. We thank French Agence Nationale de la Recherche, the AGENAVI-ITAVI SeqVol program, the INRAE Genetics Division (QuailAnnot program), the National Institute of Allergy and Infectious Diseases, National Institutes of Health, the Vallee Foundation, INRA, ALSAC, BBRSC, HFSP and NHMRC for funding support.

Authors' contributions

FM and DG contributed to the inbred quail line for sequencing. CL and DG contributed to the selection for social motivation. WW, JG, CT, PM, LH, and DB contributed to the genome sequencing and assembly. AV, FP, TJ, HK, and RL contributed to the transcriptome and annotation. LE contributed to the assembly quality assessment. AM contributed to the ERV analysis. FP, SB, and AV contributed to the selection signature analyses. TY, DB, TS, SM, AL, and MMH contributed to the photoperiod study. RW, JPS, KM, AD, HF, JS, and DB contributed to the avian flu studies. KM, JS, TY, SM, AL, MMH, DB, AV, WW, LE, AM, and RL contributed to the preparation of the manuscript. All authors read and approved the final manuscript.

Funding

HSR and LSR lines sequencing was supported by the French Agence Nationale de la Recherche (SNP-BB project, ANR-009-GENM-008). RNA sequencing of the reference individual was performed on the GeT-Plage platform (http://get.genotoul.fr/en/) and funded by the INRAE Genetics Division (QuailAnnot program). The AGENAVI-ITAVI SeqVol program for financing gallo-anseriformes genome sequencing. KMM was supported by a National Health and Medical Research Council Overseas Postdoctoral Fellowship. This work was funded in part by the National Institute of Allergy and Infectious Diseases, National Institutes of Health, under contract numbers HHSN266200700005C and HHSN272201400006C, by a young investigator award from the Vallee Foundation to JG, by ALSAC and by BB/N015347/1 and an HFSP 2015 award (RGP0030/2015).

Availability of data and materials

All data generated or analysed during this study are included in this published article (and its Additional files), or in the following public repositories. Data has been submitted to the public databses under the following accession numbers: genome sequence data, NCBI Genome [GCA_001577835.2] [123] (https://www.ncbi.nlm.nih.gov/assembly/GCA_001577835.2) and Ensembl [GCA_001577835.1] [124] (https://www.ensembl.org/Coturnix_japonica/Info/Index); transcription annotation data, SRA [PRJNA296888] [125] (https://www.ncbi.nlm.nih.gov//bioproject/PRJNA296888); RNA-seq data for infection studies, Array Express, quail [E-MTAB-3311] [126] (https://www.ebi.ac.uk/arrayexpress/experiments/E-MTAB-3311/), duck [E-MTAB-2909] [127] (https://www.ebi.ac.uk/arrayexpress/experiments/E-MTAB-2909/), chicken [E-MTAB-2908] [128] (https://www.ebi.ac.uk/arrayexpress/experiments/E-MTAB-2908/); Sequencing of HSR/LSR lines, SRA [SRP047364] [129] (https://www.ncbi.nlm.nih.gov/bioproject/PRJNA261665); RNA-seq data for photoperiod study, SRA [PRJNA490454] [130] (https://www.ncbi.nlm.nih.gov/bioproject/?term=PRJNA490454).

Ethics approval and consent to participate

ConsDD, HSR and LSR animals were bred at INRAE, UE1295 Pôle d'Expérimentation Avicole de Tours, F-37380 Nouzilly, in accordance with the European Union Guidelines for animal care, following the Council Directives 98/58/EC and 86/609/EEC. Animals were maintained under standard breeding conditions and subjected to minimal disturbance. Furthermore, the ethics committee approved the rearing protocol (authorization number 00915.02). The use of quail in photoperiod experiments were approved by the Animal Experiment Committee of Nagoya University. All experiments involving animals in the infection studies were approved by the Animal Care and Use Committee of St. Jude Children's Research Hospital and performed in compliance with relevant policies of the National Institutes of Health and the Animal Welfare Act.

Consent for publication

Not applicable

Competing interests

The authors declare that they have no competing interests.

Author details

[1]The Roslin Institute and R(D)SVS, University of Edinburgh, Easter Bush, Midlothian EH25 9RG, UK. [2]GenPhySE, Université de Toulouse, INRAE, ENVT, 31326 Castanet Tolosan, France. [3]The John Hay Building, Queensland Biosciences Precinct, 306 Carmody Road, The University of Queensland, QLD, St Lucia 4072, Australia. [4]Virology Division, Department of Infectious Diseases, St. Jude Children's Research Hospital, 262 Danny Thomas Place, Memphis, TN 38105, USA. [5]PEAT Pôle d'Expérimentation Avicole de Tours, Centre de recherche Val de Loire, INRAE, 1295 Nouzilly, UE, France. [6]Department of Developmental and Stem Cell Biology, Institut Pasteur, 25 rue du Docteur Roux, 75724, Cedex 15 Paris, France. [7]CNRS URA3738, 25 rue du Dr Roux, 75015 Paris, France. [8]McDonnell Genome Institute, Washington University School of Medicine, 4444 Forest Park Blvd, St Louis, MO 63108, USA. [9]CNRS UMR7622, Inserm U 1156, Laboratoire de Biologie du Développement, Sorbonne Université, IBPS, 75005 Paris, France. [10]Department of Radiology and Developmental Neuroscience Program, Saban Research Institute, Children's Hospital Los Angeles and Keck School of Medicine of the University of Southern California, Los Angeles, CA 90027, USA. [11]UMR85 Physiologie de la Reproduction et des Comportements, INRAE, CNRS, Université François Rabelais, IFCE, INRAE, Val de Loire, 37380 Nouzilly, Centre, France. [12]Centre for Biological Timing, Faculty of Biology, Medicine and Health, School of Medical Sciences, University of Manchester, 3.001, A.V. Hill Building, Oxford Road, Manchester M13 9PT, UK. [13]GABI, INRAE, AgroParisTech, Université Paris-Saclay, 78350 Jouy-en-Josas, France. [14]Department of Biological Production, Tokyo University of Agriculture and Technology, 3-8-1 Harumi-cho, Fuchu, Tokyo 183-8538, Japan. [15]Institute of Transformative Bio-Molecules (WPI-ITbM), Nagoya University, Furo-cho, Chikusa-ku, Nagoya 464-8601, Japan. [16]Department of Animal Sciences, Department of Surgery, Institute for Data Science and Informatics, University of Missouri, Bond Life Sciences Center, 1201 Rollins Street, Columbia, MO 65211, USA.

Received: 7 June 2019 Accepted: 24 January 2020
Published online: 12 February 2020

References

1. Shimakura K. Notes on the genetics of the Japanese quail: I. the simple, Mendelian, autosomal, recessive character, "brown-splashed white," of its plumage (in Japanese with English summary). Jpn J Genet. 1940;16:106–12.
2. Minvielle F. What are quail good for in a chicken-focused world? World's Poult Sci J. 2009;65:601–8.
3. Huss D, Poynter G, Lansford R. Japanese quail (*Coturnix japonica*) as a laboratory animal model. Lab Anim (NY). 2008;37:513–9.
4. Cheng KM, Bennett DC, Mills AD. The Japanese quail. In: Hurbrecht R, Kirkwood J, editors. UFAW handbook on the care and management of laboratory animals. 8th ed. London: Blackwell Scientific Publ; 2010.
5. Le Douarin N, Barq G. Use of Japanese quail cells as "biological markers" in experimental embryology. C R Acad Sci Hebd Seances Acad Sci D. 1969;269:1543–6.
6. Le Douarin N, Kalcheim C. The neural crest. Cambridge: Cambridge University Press; 1999.

7. Huss D, Benazeraf B, Wallingford A, Filla M, Yang J, Fraser SE, Lansford R. Transgenic quail to dynamically image amniote embryogenesis. Development. 2015;142:2850–9.
8. Bénazéraf B, Beaupeux M, Tchernooko M, Wallingford A, Salisbury T, Shirtz A, Shirtz A, Huss D, Pourquié O, François P, Lansford R. Multiscale quantification of tissue behavior during amniote embryo axis elongation. Development. 2017;144:4462–72.
9. Sato Y, Nagatoshi K, Hamano A, Imamura Y, Huss D, Nomura T, Uchida S, Lansford R. Basal filopodia and vascular mechanical stress organize fibronectin into pillars bridging the mesoderm-endoderm gap. Development. 2017;144:281–91.
10. Scott BB, Lois C. Generation of tissue-specific transgenic birds with lentiviral vectors. Proc Natl Acad Sci U S A. 2005;102:16443–7.
11. Sato Y, Poynter G, Huss D, Filla MB, Rongish BJ, Little CD, Fraser SE, Lansford R. Dynamic analysis of embryonic vascular development in transgenic quail. PLoS One. 2010;5:1–12.
12. Moreau C, Caldarelli P, Rocancourt D, Roussel J, Denans N, Pourquie O, Gros J. Timed collinear activation of hox genes during gastrulation controls the avian forelimb position. Curr Biol. 2019;29:35–50. e4
13. Huss DJ, Saias S, Hamamah S, Singh JM, Wang J, Dave M, Kim J, Eberwine J, Lansford R. Avian primordial germ cells contribute to and interact with the extracellular matrix during migration. Front Cell Dev Biol. 2019;7:35.
14. Yvernogeau L, Gautier R, Khoury H, Menegatti S, Schmidt M, Gilles JF, Jaffredo T. An in vitro model of hemogenic endothelium commitment and hematopoietic production. Development. 2016;143:1302–12.
15. Mills AD, Crawford LL, Domjan M, Faure JM. The behavior of the Japanese or domestic quail *Coturnix japonica*. Neurosci Biobehav Rev. 1997;21:261–81.
16. Adkins-Regan E. Hormones and sexual differentiation of avian social behavior. Dev Neurosci. 2009;31:342–50.
17. Meddle SL, King VM, Follett BK, Wingfield JC, Ramenofsky M, Foidart A, et al. Copulation activates Fos-like immunoreactivity in the male quail forebrain. Behav Brain Res. 1997;85:143–59.
18. Marasco V, Herzyk P, Robinson J, Spencer KA. Pre- and post-natal stress programming: developmental exposure to glucocorticoids causes long-term brain-region specific changes to transcriptome in the precocial Japanese quail. J Neuroendocrinol. 2016;28. https://doi.org/10.1111/jne.12387.
19. Mills AD, Faure JM. Divergent selection for duration of tonic immobility and social reinstatement behavior in Japanese quail (*Coturnix coturnix japonica*) chicks. J Comp Psychol. 1991;105:25–38.
20. Jones RB, Mills AD. Divergent selection for social reinstatement behaviour in Japanese quail: effects on sociality and social discrimination. Avian Biol Res. 1999;10:213–23.
21. Beaumont C, Roussot O, Feve K, Vignoles F, Leroux S, Pitel F, et al. A genome scan with AFLP markers to detect fearfulness-related QTLs in Japanese quail. Anim Genet. 2005;36:401–7.
22. Recoquillay J, Leterrier C, Calandreau L, Bertin A, Pitel F, Gourichon D, et al. Evidence of phenotypic and genetic relationships between sociality, emotional reactivity and production traits in Japanese quail. PLoS One. 2013;8:e82157.
23. Robinson JE, Follett BK. Photoperiodism in Japanese quail: the termination of seasonal breeding by photorefractoriness. Proc R Soc Lond B Biol Sci. 1982;215:95–116.
24. Nakane Y, Yoshimura T. Deep brain photoreceptors and a seasonal signal transduction cascade in birds. Cell Tissue Res. 2010;342:341–4.
25. Nakane Y, Yoshimura T. Universality and diversity in the signal transduction pathway that regulates seasonal reproduction in vertebrates. Front Neurosci. 2014;8:115.
26. Baer J, Lansford R, Cheng K. Japanese Quail as a Laboratory Animal Model. In: Fox, JG, Anderson LC, Otto GM, Pritchett-Corning KR, Whary MT, editors. Lab Animal Medicine. 3rd ed. San Diego:CA Academic Press; 2015.
27. Homma K, Jinno M, Sato K, Ando A. Studies on perfect and imperfect albinism in the Japanese quail (*Coturnix coturnix japonica*). Jpn J Zootechnical Sci. 1968;39:348–52.
28. Waligora-Dupriet AJ, Dugay A, Auzeil N, Nicolis I, Rabot S, Huerre MR, et al. Short-chain fatty acids and polyamines in the pathogenesis of necrotizing enterocolitis: kinetics aspects in gnotobiotic quails. Anaerobe. 2009;15:138–44.
29. Watanabe S, Nagayama F. Studies on the serum IgG level in Japanese quail. Jpn Poult Sci. 1979;16:59–64.
30. Shiina T, Shimizu S, Hosomichi K, Kohara S, Watanabe S, Hanzawa K, et al. Comparative genomic analysis of two avian (quail and chicken) MHC regions. J Immunol. 2004;172:6751–63.
31. Hosomichi K, Shiina T, Suzuki S, Tanaka M, Shimizu S, Iwamoto S, et al. The major histocompatibility complex (Mhc) class IIB region has greater genomic structural flexibility and diversity in the quail than the chicken. BMC Genomics. 2006;7:322.
32. Makarova NV, Ozaki H, Kida H, Webster RG, Perez DR. Replication and transmission of influenza viruses in Japanese quail. Virology. 2003;310:8–15.
33. Perez DR, Lim W, Seiler JP, Yi G, Peiris M, Shortridge KF, et al. Role of quail in the interspecies transmission of H9 influenza A viruses: molecular changes on HA that correspond to adaptation from ducks to chickens. J Virol. 2003;77:3148–56.
34. Wan H, Perez DR. Quail carry sialic acid receptors compatible with binding of avian and human influenza viruses. Virology. 2006;346:278–86.
35. Guan Y, Peiris JS, Lipatov AS, Ellis TM, Dyrting KC, Krauss S, et al. Emergence of multiple genotypes of H5N1 avian influenza viruses in Hong Kong SAR. Proc Natl Acad Sci U S A. 2002;99:8950–5.
36. Webster RG, Guan Y, Peiris M, Walker D, Krauss S, Zhou NN, et al. Characterization of H5N1 influenza viruses that continue to circulate in geese in southeastern China. J Virol. 2002;76:118–26.
37. Maccallum I, Przybylski D, Gnerre S, Burton J, Shlyakhter I, Gnirke A, et al. ALLPATHS 2: small genomes assembled accurately and with high continuity from short paired reads. Genome Biol. 2009;10:R103.
38. Oldeschulte DL, Halley YA, Wilson ML, Bhattarai EK, Brashear W, Hill J, et al. Annotated draft genome assemblies for the Northern Bobwhite (*Colinus virginianus*) and the Scaled Quail (*Callipepla squamata*) reveal disparate estimates of modern genome diversity and historic effective population size. G3 (Bethesda). 2017;7:3047–58.
39. Wu Y, Zhang Y, Hou Z, Fan G, Pi J, Sun S, et al. Population genomic data reveal genes related to important traits of quail. Gigascience. 2018;7:giy049.
40. Morgulis A, Gertz EM, Schäffer AA, Agarwala R. WindowMasker: window-based masker for sequenced genomes. Bioinformatics. 2006;22:134–41.
41. Altschul SF, Gish W, Miller W, Myers EW, Lipman DJ. Basic local alignment search tool. J Mol Biol. 1990;215:403–10.
42. Zdobnov EM, Tegenfeldt F, Kuznetsov D, Waterhouse RM, Simão FA, Ioannidis P, et al. OrthoDB v9.1: cataloging evolutionary and functional annotations for animal, fungal, plant, archaeal, bacterial and viral orthologs. Nucleic Acids Res. 2017;45:D744–9.
43. Waterhouse RM, Seppey M, Simão FA, Manni M, Ioannidis P, Klioutchnikov G, et al. BUSCO applications from quality assessments to gene prediction and Phylogenomics. Mol Biol Evol. 2017;35:543–8.
44. Warren WC, Hillier LW, Tomlinson C, Minx P, Kremitzki M, Graves T, et al. A new chicken genome assembly provides insight into avian genome structure. G3 (Bethesda). 2017;7:109–17.
45. van Tuinen M, Dyke GJ. Calibration of galliform molecular clocks using multiple fossils and genetic partitions. Mol Phylogenet Evol. 2004;30:74–86.
46. Dalloul RA, Long JA, Zimin AV, Aslam L, Beal K, Blomberg LA, et al. Multi-platform next-generation sequencing of the domestic Turkey (*Meleagris gallopavo*): genome assembly and analysis. PLoS Biol. 2010;8:e1000475.
47. Griffin DK, Robertson LB, Tempest HG, Vignal A, Fillon V, Crooijmans RP, et al. Whole genome comparative studies between chicken and Turkey and their implications for avian genome evolution. BMC Genomics. 2008;9:168.
48. Kapusta A, Suh A, Feschotte C. Dynamics of genome size evolution in birds and mammals. Proc Natl Acad Sci U S A. 2017;114:E1460–9.
49. Mason AS, Fulton JE, Hocking PM, Burt DW. A new look at the LTR retrotransposon content of the chicken genome. BMC Genomics. 2016;17:688.
50. Kapusta A, Suh A. Evolution of bird genomes-a transposons-eye view. Ann N Y Acad Sci. 2017;1389:164–85.
51. Varela M, Spencer TE, Palmarini M, Arnaud F. Friendly viruses. Ann N Y Acad Sci. 2009;1178:157–72.
52. Aswad A, Katzourakis A. Paleovirology and virally derived immunity. Trends Ecol Evol. 2012;27:627–36.
53. Recoquillay J, Pitel F, Arnould C, Leroux S, Dehais P, Moréno C, et al. A medium density genetic map and QTL for behavioral and production traits in Japanese quail. BMC Genomics. 2015;16:10.
54. Fariello MI, Boitard S, Mercier S, Robelin D, Faraut T, Arnould C, et al. Accounting for linkage disequilibrium in genome scans for selection without individual genotypes: the local score approach. Mol Ecol. 2017;26:3700–14.
55. Bonhomme M, Chevalet C, Servin B, Boitard S, Abdallah J, Blott S, et al. Detecting selection in population trees: the Lewontin and Krakauer test extended. Genetics. 2010;186:241–62.
56. Nakajima J, Okamoto N, Tohyama J, Kato M, Arai H, Funahashi O, et al. De novo EEF1A2 mutations in patients with characteristic facial features, intellectual disability, autistic behaviors and epilepsy. Clin Genet. 2015;87:356–61.

57. Kleefstra T, Brunner HG, Amiel J, Oudakker AR, Nillesen WM, Magee A, et al. Loss-of-function mutations in euchromatin histone methyl transferase 1 (EHMT1) cause the 9q34 subtelomeric deletion syndrome. Am J Hum Genet. 2006;79:370–7.
58. Balemans MC, Huibers MM, Eikelenboom NW, Kuipers AJ, van Summeren RC, Pijpers MM, et al. Reduced exploration, increased anxiety, and altered social behavior: autistic-like features of euchromatin histone methyltransferase 1 heterozygous knockout mice. Behav Brain Res. 2010;208:47–55.
59. Mitra AK, Dodge J, Van Ness J, Sokeye I, Van Ness BA. De novo splice site mutation in EHMT1 resulting in Kleefstra syndrome with pharmacogenomics screening and behavior therapy for regressive behaviors. Mol Genet Genomic Med. 2017;5:130–40.
60. Roppongi RT, Karimi B, Siddiqui TJ. Role of LRRTMs in synapse development and plasticity. Neurosci Res. 2017;116:18–28.
61. Ralph C, Hedlund L, Murphy WA. Diurnal cycles of melatonin in bird pineal bodies. Comp Biochem Physiol. 1967;22:591–9.
62. Lynch HJ. Diurnal oscillations in pineal melatonin content. Life Sci 1. 1971;10:791–5.
63. Cockrem JF, Follett BK. Circadian rhythm of melatonin in the pineal gland of the Japanese quail (*Coturnix coturnix japonica*). J Endocrinol. 1985;107:317–24.
64. Wood S, Loudon A. Clocks for all seasons: unwinding the roles and mechanisms of circadian and interval timers in the hypothalamus and pituitary. J Endocrinol. 2014;222:R39–59.
65. Menaker M. Extraretinal light perception in the sparrow. I. Entrainment of the biological clock. Proc Natl Acad Sci U S A. 1968;59:414–21.
66. Yoshimura T. Thyroid hormone and seasonal regulation of reproduction. Front Neuroendocrinol. 2013;34:157–66.
67. Yasuo S, Watanabe M, Okabayashi N, Ebihara S, Yoshimura T. Circadian clock genes and photoperiodism: comprehensive analysis of clock gene expression in the mediobasal hypothalamus, the suprachiasmatic nucleus, and the pineal gland of Japanese quail under various light schedules. Endocrinology. 2003;144:3742–8.
68. Haas R, Alenciks E, Meddle S, Fraley GS. Expression of deep brain photoreceptors in the Pekin drake: a possible role in the maintenance of testicular function. Poult Sci. 2017;96:2908–19.
69. Nakane Y, Ikegami K, Ono H, Yamamoto N, Yoshida S, Hirunagi K, et al. A mammalian neural tissue opsin (Opsin 5) is a deep brain photoreceptor in birds. Proc Natl Acad Sci U S A. 2010;107:15264–8.
70. García-Fernández JM, Cernuda-Cernuda R, Davies WI, Rodgers J, Turton M, Peirson SN, et al. The hypothalamic photoreceptors regulating seasonal reproduction in birds: a prime role for VA opsin. Front Neuroendocrinol. 2015;37:13–28.
71. Chowdhury VS, Yamamoto K, Ubuka T, Bentley GE, Hattori A, Tsutsui K. Melatonin stimulates the release of gonadotropin-inhibitory hormone by the avian hypothalamus. Endocrinology. 2010;151:271–80.
72. Cozzi B, Stankov B, Viglietti-Panzica C, Capsoni S, Aste N, Lucini V, et al. Distribution and characterization of melatonin receptors in the brain of the Japanese quail, *Coturnix japonica*. Neurosci Lett. 1993;150:149–52.
73. Lincoln G, Messager S, Andersson H, Hazlerigg D. Temporal expression of seven clock genes in the suprachiasmatic nucleus and the pars tuberalis of the sheep: evidence for an internal coincidence timer. Proc Natl Acad Sci U S A. 2002;99:13890–5.
74. Yasuo S, Watanabe M, Tsukada A, Takagi T, Iigo M, Shimada K, et al. Photoinducible phase-specific light induction of Cry1 gene in the Pars Tuberalis of Japanese quail. Endocrinology. 2004;145:1612–6.
75. Ikegami K, Atsumi Y, Yorinaga E, Ono H, Murayama I, Nakane Y, et al. Low temperature-induced circulating triiodothyronine accelerates seasonal testicular regression. Endocrinology. 2015;156:647–59.
76. Millar RP, Newton CL, Roseweir AK. Chapter 2 - Neuroendocrine GPCR Signaling. In: Fink G, Pfaff DW, Levine JE, editors. Handbook of neuroendocrinology. Cambridge: Academic Press; 2012. p. 21–53.
77. Shichida Y, Matsuyama T. Evolution of opsins and phototransduction. Philos Trans R Soc B Biol Sci. 2009;364:2881–95.
78. Hase M, Yokomizo T, Shimizu T, Nakamura M. Characterization of an orphan G protein-coupled receptor, GPR20, that constitutively activates Gi proteins. J Biol Chem. 2008;283:12747–55.
79. Pinzon-Rodriguez A, Bensch S, Muheim R. Expression patterns of cryptochrome genes in avian retina suggest involvement of Cry4 in light-dependent magnetoreception. J R Soc Interface. 2018;15:20180058.
80. Zoltowski BD, Chelliah Y, Wickramaratne A, Jarocha L, Karki N, Xu W, et al. Chemical and structural analysis of a photoactive vertebrate cryptochrome from pigeon. Proc Natl Acad Sci U S A. 2019;116:19449–57.
81. Kato M, Sugiyama T, Sakai K, Yamashita T, Fujita H, Sato K, et al. Two opsin 3-related proteins in the chicken retina and brain: a TMT-type opsin 3 is a blue-light sensor in retinal horizontal cells, hypothalamus, and cerebellum. PLoS One. 2016;11:e0163925.
82. Salomonsen J, Chattaway JA, Chan AC, Parker A, Huguet S, Marston DA, et al. Sequence of a complete chicken BG haplotype shows dynamic expansion and contraction of two gene lineages with particular expression patterns. PLoS Genet. 2014;10:e1004417.
83. Cheng Y, Prickett MD, Gutowska W, Kuo R, Belov K, Burt DW. Evolution of the avian β-defensin and cathelicidin genes. BMC Evol Biol. 2015;15:188.
84. Barber MR, Aldridge JR Jr, Webster RG, Magor KE. Association of RIG-I with innate immunity of ducks to influenza. Proc Natl Acad Sci U S A. 2010;107:5913–8.
85. Magor KE, Miranzo Navarro D, Barber MR, Petkau K, Fleming-Canepa X, Blyth GA, et al. Defense genes missing from the flight division. Dev Comp Immunol. 2013;41:377–88.
86. Bertran K, Dolz R, Busquets N, Gamino V, Vergara-Alert J, Chaves AJ, et al. Pathobiology and transmission of highly and low pathogenic avian influenza viruses in European quail (*Coturnix c. coturnix*). Vet Res. 2013;44:23.
87. Nguyen TH, Than VT, Thanh HD, Hung VK, Nguyen DT, Kim W. Intersubtype reassortments of H5N1 highly pathogenic avian influenza viruses isolated from quail. PLoS One. 2016;11:e0149608.
88. Cornelissen JB, Vervelde L, Post J, Rebel JM. Differences in highly pathogenic avian influenza viral pathogenesis and associated early inflammatory response in chickens and ducks. Avian Pathol. 2013;42:347–64.
89. Smith J, Smith N, Yu L, Paton IR, Gutowska MW, Forrest HL, et al. A comparative analysis of host responses to avian influenza infection in ducks and chickens highlights a role for the interferon-induced transmembrane proteins in viral resistance. BMC Genomics. 2015;16:574.
90. Theocharidis A, van Dongen S, Enright AJ, Freeman TC. Network visualization and analysis of gene expression data using BioLayout express (3D). Nat Protoc. 2009;4:1535–50.
91. Kuchipudi SV, Dunham SP, Nelli R, White GA, Coward VJ, Slomka MJ, et al. Rapid death of duck cells infected with influenza: a potential mechanism for host resistance to H5N1. Immunol Cell Biol. 2010;90:116–23.
92. Amini-Bavil-Olyaee S, Choi YJ, Lee JH, Shi M, Huang IC, Farzan M, et al. The antiviral effector IFITM3 disrupts intracellular cholesterol homeostasis to block viral entry. Cell Host Microbe. 2013;13:452–64.
93. Rutter M. Diagnosis and definition of childhood autism. J Autism Child Schizophr. 1978;8:139–61.
94. American Psychiatric Association. Diagnostic and Statistical Manual of Mental Disorders. 4th ed. Washington DC: 2000.
95. Francois N, Mills AD, Faure JM. Inter-individual distances during open-field tests in Japanese quail (*Coturnix japonica*) selected for high or low levels of social reinstatement behaviour. Behav Process. 1999;47:73–80.
96. Schweitzer C, Houdelier C, Lumineau S, Levy F, Arnould C. Social motivation does not go hand in hand with social bonding between two familiar Japanese quail chicks Coturnix japonica. Anim Behav. 2009;79:571–8.
97. Francois N, Decros S, Picard M, Faure JM, Mills AD. Effect of group disruption on social behaviour in lines of Japanese quail (*Coturnix japonica*) selected for high or low levels of social reinstatement behaviour. Behav Process. 2000;48:171–81.
98. Minvielle F, Monvoisin JL, Costa J, Frénot A, Maeda Y. Changes in heterosis under within-line selection or reciprocal recurrent selection: an experiment on early egg production in Japanese quail. J Anim Breed Genet. 1999;116:363–77.
99. Roussot O, Feve K, Plisson-Petit F, Pitel F, Faure JM, Beaumont C, et al. AFLP linkage map of the Japanese quail *Coturnix japonica*. Genet Sel Evol. 2003; 35:559–72.
100. English AC, Richards S, Han Y, Wang M, Vee V, Qu J, et al. Mind the gap: upgrading genomes with Pacific Biosciences RS long-read sequencing technology. PLoS One. 2012;7:e47768.
101. Boetzer M, Pirovano W. SSPACE-LongRead: scaffolding bacterial draft genomes using long read sequence information. BMC Bioinform. 2014;15:211.
102. Thibaud-Nissen F, Souvorov A, Murphy T, DiCuccio M, Kitts P. Eukaryotic Genome Annotation Pipeline. In: The NCBI Handbook [Internet], 2nd edn. 2013. p. 133–56.
103. Stanke M, Keller O, Gunduz I, Hayes A, Waack S, Morgenstern B. AUGUSTUS: ab initio prediction of alternative transcripts. Nucleic Acids Res. 2006;34:W435–9.
104. Eddy SR. Profile hidden Markov models. Bioinformatics. 1998;14:755–63.
105. Derrien T, André C, Galibert F, Hitte C. AutoGRAPH: an interactive web server for automating and visualizing comparative genome maps. Bioinformatics. 2007;23:498–9.
106. Kumar S, Stecher G, Tamura K. MEGA7: molecular evolutionary genetics analysis version 7.0 for bigger datasets. Mol Biol Evol. 2016;33:1870–4.

107. Saitou N, Nei M. The neighbor-joining method: a new method for reconstructing phylogenetic trees. Mol Biol Evol. 1987;4:406–25.
108. McCarthy EM, McDonald JF. LTR_STRUC: a novel search and identification program for LTR retrotransposons. Bioinformatics. 2003;19:362–7.
109. Ellinghaus D, Kurtz S, Willhoeft U. LTRharvest, an efficient and flexible software for de novo detection of LTR retrotransposons. BMC Bioinform. 2008;9:18.
110. Rho M, Choi JH, Kim S, Lynch M, Tang H. De novo identification of LTR retrotransposons in eukaryotic genomes. BMC Genomics. 2007;8:90.
111. Smit A, Hubley R, Green P. RepeatMasker Open-4.0.3. 2013. http://repeatmasker.org. Accessed 20 Feb 2018.
112. Li H, Durbin R. Fast and accurate short read alignment with Burrows-Wheeler transform. Bioinformatics. 2009;25:1754–60.
113. Boitard S, Kofler R, Francoise P, Robelin D, Schlotterer C, Futschik A. Pool-hmm: a Python program for estimating the allele frequency spectrum and detecting selective sweeps from next generation sequencing of pooled samples. Mol Ecol Resour. 2013;13:337–40.
114. Kim D, Pertea G, Trapnell C, Pimentel H, Kelley R, Salzberg SL. TopHat2: accurate alignment of transcriptomes in the presence of insertions, deletions and gene fusions. Genome Biol. 2013;14:R36.
115. Liao Y, Smyth GK, Shi W. featureCounts: an efficient general-purpose program for assigning sequence reads to genomic features. Bioinformatics. 2014;30:923–30.
116. Liao Y, Smyth GK, Shi W. The subread aligner: fast, accurate and scalable read mapping by seed-and-vote. Nucleic Acids Res. 2013;41:e108.
117. Law CW, Chen Y, Shi W, Smyth GK. Voom: precision weights unlock linear model analysis tools for RNA-seq read counts. Genome Biol. 2014;15:R29.
118. Benjamini Y, Hochberg Y. Controlling the false discovery rate: a practical and powerful approach to multiple testing. J R Stat Soc Ser B Methodol. 1995;57:289–300.
119. Bray NL, Pimentel H, Melsted P, Pachter L. Near-optimal probabilistic RNA-seq quantification. Nat Biotechnol. 2016;4:525–7.
120. Trapnell C, Williams BA, Pertea G, Mortazavi A, Kwan G, van Baren MJ, et al. Transcript assembly and quantification by RNA-Seq reveals unannotated transcripts and isoform switching during cell differentiation. Nat Biotechnol. 2010;28:511–5.
121. Pertea M, Pertea GM, Antonescu CM, Chang TC, Mendell JT, Salzberg SL. StringTie enables improved reconstruction of a transcriptome from RNA-seq reads. Nat Biotechnol. 2015;33:290–5.
122. Thomas PD, Campbell MJ, Kejariwal A, Mi H, Karlak B, Daverman R, et al. PANTHER: a library of protein families and subfamilies indexed by function. Genome Res. 2003;13:2129–41.
123. Morris KM, Hindle MM, Boitard S, Burt DW, Danner AF, Eory L, et al. The quail as an avian model system: its genome provides insights into social behaviour, seasonal biology and infectious disease response. Supporting Dataset. NCBI GCA_001577835.1 (https://www.ncbi.nlm.nih.gov/assembly/GCA_001577835.2). Accessed 17 Jan 2020.
124. Morris KM, Hindle MM, Boitard S, Burt DW, Danner AF, Eory L, et al. The quail as an avian model system: its genome provides insights into social behaviour, seasonal biology and infectious disease response. Supporting Dataset. Ensembl GCA_001577835.1 (https://www.ensembl.org/Coturnix_japonica/Info/Index). Accessed 17 Jan 2020.
125. Morris KM, Hindle MM, Boitard S, Burt DW, Danner AF, Eory L, et al. Coturnix japonica strain: Cons DD Transcriptome or Gene expression. SRA PRJNA296888 (https://www.ncbi.nlm.nih.gov//bioproject/PRJNA296888). Accessed 17 Jan 2020.
126. Smith J. E-MTAB-3311 - Infection of quail with avian influenza H5N1 and H5N2 viruses. ArrayExpress E-MTAB-3311 (https://www.ebi.ac.uk/arrayexpress/experiments/E-MTAB-3311). Accessed 17 Jan 2020.
127. Smith J. E-MTAB-2909 - RNA-seq of lung and ileum samples at 1 and 3 days post infection (dpi) from ducks infected with either low pathogenic (H5N2) or highly pathogenic (H5N1) avian influenza. ArrayExpress E-MTAB-2909 (https://www.ebi.ac.uk/arrayexpress/experiments/E-MTAB-2909). Accessed 17 Jan 2020.
128. Smith J. E-MTAB-2908 - RNA-seq of lung and ileum samples at 1 and 3 days post infection (dpi) from chickens infected with either low pathogenic (H5N2) or highly pathogenic (H5N1) avian influenza. ArrayExpress E-MTAB-2908 (https://www.ebi.ac.uk/arrayexpress/experiments/E-MTAB-2908). Accessed 17 Jan 2020.
129. Pitel F. *Coturnix coturnix* strain: HSR genome sequencing. SRA PRJNA261665 (https://www.ncbi.nlm.nih.gov/bioproject/PRJNA261665). Accessed 17 Jan 2020.
130. Hindle M. Coturnix japonica (Japanese quail), Evolution of seasonal timers. SRA PRJNA490454 (https://www.ncbi.nlm.nih.gov/bioproject/?term=PRJNA490454). Accessed 17 Jan 2020.

Publisher's Note

Springer Nature remains neutral with regard to jurisdictional claims in published maps and institutional affiliations.

Ready to submit your research? Choose BMC and benefit from:

- fast, convenient online submission
- thorough peer review by experienced researchers in your field
- rapid publication on acceptance
- support for research data, including large and complex data types
- gold Open Access which fosters wider collaboration and increased citations
- maximum visibility for your research: over 100M website views per year

At BMC, research is always in progress.

Learn more biomedcentral.com/submissions